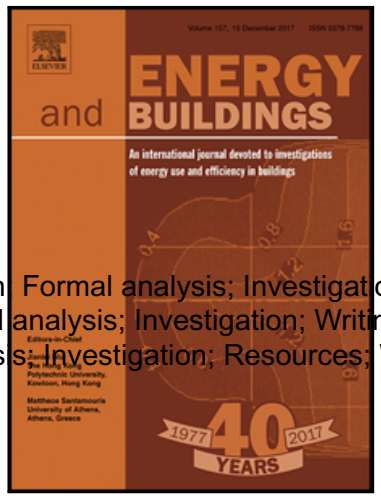

Effects of climate change on variations in climatic zones and heating energy consumption of residential buildings in the southern Chile

Konstantin Verichev Conceptualization; Methodology; Software; Validation; Formal analysis; Investigation; Resourc
Montserrat Zamorano Conceptualization; Methodology; Validation; Formal analysis; Investigation; Writing - review
Manuel Carpio Conceptualization; Methodology; Validation; Formal analysis; Investigation; Resources; Writing - re

PII: S0378-7788(19)33042-7
DOI: https://doi.org/10.1016/j.enbuild.2020.109874
Reference: ENB 109874

To appear in: *Energy & Buildings*

Received date: 4 October 2019
Revised date: 12 January 2020
Accepted date: 14 February 2020

Please cite this article as: Konstantin Verichev Conceptualization; Methodology; Software; Validation; Formal analys
Montserrat Zamorano Conceptualization; Methodology; Validation; Formal analysis; Investigation; Writing - review
Manuel Carpio Conceptualization; Methodology; Validation; Formal analysis; Investigation; Resources; Writing - re
Effects of climate change on variations in climatic zones and heating energy consumption of residential buildings in the southern Chile, *Energy & Buildings* (2020), doi: https://doi.org/10.1016/j.enbuild.2020.109874

Highlights

- In the future, climate zones for building will mostly be replaced by warmer ones
- A decrease in future heating energy consumption has been identified
- The impossibility of using actual building norms in the future was demonstrated

Effects of climate change on variations in climatic zones and heating energy consumption of residential buildings in the southern Chile

Konstantin Verichev [a, b, c], Montserrat Zamorano [a, d], Manuel Carpio [c, e *]
[a] *Department of Civil Engineering, University of Granada, Severo Ochoa S/N, Granada, Spain*
[b] *Institute of Civil Engineering, Universidad Austral de Chile, General Lagos 2050, Valdivia, Chile*
[c] *Department of Construction Engineering and Management, School of Engineering, Pontificia, Universidad Católica de Chile, Avenida Vicuña Mackenna 4860, Santiago, Chile*
[d] *PROMA, Proyectos de Ingeniería Ambiental, S.L., Granada, Spain*
[e] *UC Energy Research Center, Pontificia Universidad Católica de Chile, Avenida Vicuña Mackenna 4860, Santiago, Chile*
**Corresponding author: manuel.carpio@ing.puc.cl*

Abstract
Global climate change is changing meteorological parameters and climate zones for building in different parts of the world, as well as changing energy consumption by dwellings. Therefore, in this study, changes in climatic zones for building in three regions in southern Chile have been analysed under the conditions of two future climatic scenarios (RCP2.6 and RCP8.5). On average, the temperature will increase by +0.68°C and +1.51°C by 2050–2065 in the study region for scenarios RCP2.6 and RCP8.5, respectively. This will cause a decrease in the annual heating degree-days values. In 72% of cities (RCP2.6) and in 92% of cities (RCP8.5), climate zones for building will be replaced by warmer ones. Consequently, the possibility of applying the current building standard of the country in future climatic conditions has been questioned. Finally, it was found that the heating energy consumption of a single-family house will decrease by 13% and 27% on average for the RCP2.6 and RCP8.5 scenarios, respectively.

Keywords
energy; mapping; climatic zoning; climate change; building; heating

Nomenclature

AR5 – The 5th Assessment Report of IPCC
CCRR – Center for Climate and Resilience Research
EC – Energy Consumption
GBS – Green Building Studio
GHG – Greenhouse Gases
HDD15°C – heating degree-days with base temperature 15°C
IPCC – Intergovernmental Panel on Climate Change
MM5 – Mesoscale Meteorological Model Version 5
OGUC – General Ordinance of Urban Planning and Housing of the Ministry of Housing and Urban Development of Chile
RCP – Representative Concentration Pathways of IPCC
RF_{tot} – The total Radiative Forcing
RT – Thermal Regulation Application Manual of the OGUC
SRES –The Special Report on Emissions Scenarios of IPCC
U-value – Thermal transmittance, [$W/m^2 \cdot K$]

1. Introduction

The Intergovernmental Panel on Climate Change (IPCC) is a United Nations (UN) organisation established to assess the risk of the unequivocal global climate change caused by factors created by human actions [1]. In order to make projections of a possible future climate change, the IPCC published "The Special Report on Emissions Scenarios" (SRES) [2]. This document describes a series of greenhouse gas (GHG) emission scenarios, based on different situations of global socio-economic development, which were incorporated into the 3rd Assessment Report of IPCC in 2001 [3] and in the 4th Assessment Report of IPCC in 2007 [4]. The established scenarios, and their characteristics are as follows:

(i) **A1**; of very rapid economic development. It includes three specifications:
   a. **A1FI**; where the use of fossil fuels will prevail;
   b. **A1B**; with balance of energy sources; and
   c. **A1T**; where the use of non-fossil fuels will prevail.

(ii) **A2**; of the heterogeneous world with less concern for rapid economic development, with regional differences in economic development.

(iii) **B1**; of the convergent world with rapid changes in structure of economy (prevalence of service and information), reduction in material consumption, introduction of clean processes and technologies.

(iv) **B2**; focused on sustainability, local solutions for environmental and economic problems, less rapid and more diverse technological change, intermediate economic development.

In order to incorporate new scenarios and develop climatic models that improve our knowledge of the physical and chemical processes of the planet's climate system, the 5th Assessment Report of IPCC (AR5) was published in 2013 [1]. In this document the main quantitative parameter that describes climate change is the total Radiative Forcing (RF_{tot}), whose value is positive and has led to the absorption of energy by the climatic system. The main contribution to RF_{tot} comes from the increase in the CO_2 concentration in the atmosphere produced since 1750. The anthropogenic RF_{tot} in 2011, in relation to 1750, was 2.29 Wm^{-2}, and has increased more rapidly since 1970 than in the previous decades [1]. Consequently, for the IPCC AR5, the scientific community has defined a set of four scenarios, called Representative Concentration Pathways (RCP), which are characterised by the approximate calculation they make of the RF_{tot} in the year 2100 in relation to the year 1750:

(i) **RCP2.6**; this mitigation scenario shows negative emissions from energy use in the second half of the 21st century. Cumulative emissions of GHG from 2010 to 2100 need to be reduced by 70%, requiring substantial changes in energy use and emissions of non-CO_2 gases (prescribed CO_2 concentration of 421 ppm and RF_{tot} = 2.6 Wm^{-2} in 2100). These measures (specifically the use of bio-energy and reforestation measures) have clear consequences for global land use. Every country must accept climate change policies [1,5,6].

(ii) **RCP4.5**; stabilisation scenario with peak of population of 9 billion inhabitants in 2065 and with prognostic population of 8.7 billion in 2100. The imperative to limit emissions in order to reach this target drives changes in the energy system, including shifts to electricity, to lower-emission energy technologies and to the deployment of carbon capture and geologic storage technology. (The growth of emissions of CO_2 by 2035 from energy and industrial sources, and then a decline). The RCP4.5 emissions price also applies to land use emissions; as a result, forest

lands expand from their present day extent. Prescribed CO_2 concentrations of 538 ppm and RF_{tot} = 4.5 Wm^{-2} in 2100 [1,7].

(iii) **RCP6.0**; stabilisation scenario with a peak of population of 9.8 billion between 2080 and 2090. GHG emissions of RCP6 peak around 2060 and then decline through the rest of the century. The energy intensity improvement rates change from 0.9% per year to 1.5% per year around 2060. Emissions are assumed to be reduced cost-effectively in any period through a global market for emissions permits. Prescribed CO_2 concentration of 670 ppm and RF_{tot} = 6.0 Wm^{-2} in 2100 [1,8].

(iv) **RCP8.5**; scenario with very high GHG emission. The RCP8.5 combines assumptions about high population (12 billion in 2100) and relatively slow income growth with modest rates of technological change and energy intensity improvements, leading in the long term to high energy demand and GHG emissions in absence of climate change policies. Prescribed CO_2 concentration of 936 ppm and RF_{tot} = 8.5 Wm^{-2}in 2100 [1,9].

According to AR5 [1], a graph of conformity between the SRES and RCP emission scenarios with RFtot values for the 21st century is presented in Fig. 1. It can be seen that the SRES A2 scenario, in the middle of the century, is not as strong as RCP8.5, but by 2100 these two scenarios are similar in the context of radiative effect to the Earth's climatic system. For B1 corresponding to scenario RCP4.5 and scenario RCP2.6 there is no analogue in the SRES system.

In AR5 the authors note that: “RCP scenarios are new ones that specify concentrations and corresponding emissions but are not directly based on socio-economic storylines like the SRES scenarios. The RCP scenarios are based on a different approach and include more consistent short-lived gases and land use changes. They are not necessarily more capable of representing future developments than the SRES scenarios”. Therefore, the equivalent use of RCP or SRES scenarios in scientific research is appropriate.

In the context of global warming, special attention has been given to the evaluation of the effects of temperature increase in different geographical areas and in different sectors of economic activity, including building and its relationship to energy consumption (EC) [10–13]. Most of these studies focus on evaluating changes in the EC of residential buildings for heating and cooling, as well as the interior thermal comfort in different parts of the world.

To evaluate changes in heating and cooling EC of residential buildings, different techniques for approximating future climatic conditions were used [14–18]. Thus, in the work of Gaterell and McEvoy (2005) [16], it is assumed that the Milan weather file used to represent the UK climate in 2050 under the low emissions climate scenario and Rome for the UK climate by 2050 under the high emissions climate scenario. Studies have been conducted in which the effects of climate change on heating/cooling EC have been analysed [19–21] on the basis of indoor temperature and thermal comfort [22–24] and building adaptation methods in climate change conditions [20,23,25] based on scenarios developed by local meteorological institutes such as the United Kingdom Climate Impacts Program (UKCIP), the Royal Netherlands Meteorological Institute in the Netherlands [26], the Environment Agency of Abu-Dhabi and the Ministry of Energy in United Arab Emirates [27], the National Institute for Environmental Studies and Agency for Marine-Earth Science and Technology of Japan [28,29]. After 2014, articles on the evaluation of changes in heating and cooling EC and change of interior thermal comfort of residential dwellings, under the SRES and RCP scenarios, have been published. Table 1 shows a summary of the publications reviewed,

where it can be seen how the scenario A2 is more popular and reflected in a large number of scientific papers. It is also observed that SRES scenarios are used more; this can be justified because they have been operating since 2001 and because of their socioeconomic understanding. However, in recent years there has been an increase in the use of RCP scenarios in scientific papers. A fairly wide geographical distribution of the works is also seen. SRES scenarios were used in research for countries such as Finland [30], Hong Kong [31], Bangladesh [32], Turkey [33], Taiwan [34], Australia [35], Brazil [36,37], USA [38–40], Canada [41], Argentina [42], and RCP scenarios in Sweden [43], France [44], Portugal [45], Brazil [46], USA [47,48], Italy [49] and Argentina [50].

It can be summarised that most of the scientific works are oriented to the analysis of the effects of climate change on cooling and heating EC in the future. To a lesser extent, studies are presented on the evaluation of changes in climatic zones for building, concluding that in the future, for all geographical regions, the heating EC of buildings will decrease and the cooling EC will increase in conjunction with an increase in days of interior thermal discomfort. For example, in Greece, by 2100, it is possible that the heating EC of buildings will decrease by 50%, while the cooling EC of buildings will increase up to 248% [11]. In the case of the evaluation of climate change effects on building construction, it is observed that most of them correspond to studies of single-family residential dwellings; however, there are studies in which buildings of other types have been analysed, such as schools, hotels, high-rise apartments [56] and offices. In the latter case they have spread to countries like the USA [56], Hong Kong [51], Australia [57], Greece [52], Spain [54], China [55], Austria [58,59], Germany, Greece and Australia [53].

A limited number of meteorological data and the focus on national building codes cause almost all of the studies carried out to be directed to a certain number of cities or geographical points and there are not many that analyse the changes of climatic zones for building and spatial distribution of theoretical EC in large geographical areas, such as in studies of cartographic analysis of real and theoretical EC of the dwellings [60–62].

In the case of Chile, the heating and cooling EC in different types of buildings such as office buildings has been analysed for the years 2020, 2050 and 2080 under the influence of A2 climate change scenario in nine cities [63]. A study has also been published in which interior comfort in a social residential building in the city of Concepcion and the change of comfort for scenario A2 were analysed. [64]. Finally, the change of thermal zones (synonymous with climatic zones) for building in three regions of southern Chile has been studied based on data of the last decade from 35 meteorological stations [65].

In the present study we analyse the evolution of the existing climatic zones for building in climate change conditions in order to analyse the conformity level of the present regulations to future climatic conditions and to estimate possible future changes in the heating EC of a single-family dwelling in a fairly large geographical area. To this end, the main objective of this work is the estimation of: (i) thermal zones for building and (ii) heating EC in the southern part of Chile in different climate change scenarios through high spatial resolution meteorological data, energy simulation and specific methodology for the evaluation of future changes.

2. Material and methods

This section presents the tools, study area, national building regulations and methodologies used in this study.

2.1. Computational tools used

This section describes the software used in the present research, its main functions and licensing:

- **3D modeling of structural and architectural components**. The Building Information Modeling (BIM) methodology was used, through the Revit software of the Autodesk® version 2018, licensed by the *Universidad Austral de Chile*. Revit allows the possibility to make a 3D model of the house and convert it into a gbXML file to later perform an energy analysis using an energy simulation tool.
- **Energetic simulation.** The Green Building Studio (GBS), version 2018.99.46.101 (DOE-2.2-48r) (Autodesk®) associated with the Revit license was used. The results of GBS energy modelling were compared with results of other energy simulation tools [66–73] and were used in various scientific works [74–82]. In the general case for the EC analysis of a dwelling, more detailed and accurate modelling BIM tools can be used [83]. GBS energy simulation is based on data from the Mesoscale Meteorological Model ver.5 (MM5) data from 2006, with a 12.7 km spatial resolution [84]. MM5 data contains hourly values of dry-bulb temperature, dew point temperature, atmospheric pressure, relative humidity, wind speed, wind direction, total sky cover, and components of solar radiation. In our investigation, due to the studied area´s extension, using GBS is correct for EC modelling because it is necessary to have high spatial resolution EC simulation results and cover a fairly large geographical area.
- **Mapping.** ArcGIS 10.5 [85]. Licensed by the *Pontificia Universidad Católica de Chile*.
- **Statistical analysis.** The IBM SPSS Statistics software ver. 22.0 licensed by the *Pontificia Universidad Católica de Chile* was used.

2.2. Study area

Fig. 2a shows the study area comprising three regions in southern Chile, framed between latitudes 37.5°S and 44.1°S: La Araucanía region, Los Ríos region and Los Lagos region, whose capitals are Temuco, Valdivia and Puerto Montt, respectively. The regions of La Araucanía, Los Ríos and Los Lagos contain 32, 12 and 30 communes, respectively (grey borders within the regions) and the principal cities of communes are presented on the maps (Fig. 2b-d). The total area of these three regions is 98,885 km^2, with approximately two million inhabitants [86].

The orography of the study area (from the north to Puerto Montt city) is characterised by the presence of the Coastal Mountain Range with heights of up to 1,000 m, an intermediate depression with heights of up to 300 m and the Andes Mountain Range with heights of up to 3,000 m. To the south of the continental part of the Los Lagos region is Chiloé Island (southwest) with heights of up to 800 m and the continuation of the Andes Mountain Range (southeast) [87].

On the Pacific coast, when moving from north to south, the maximum temperatures of the hottest months vary from 21°C to 18°C. In the Andes Mountains, the maximum temperatures vary from 30°C to 16°C, while the minimum temperatures of the coldest months vary between -2°C and -5°C. In the northern part of the Pacific coast, minimum temperatures vary in the range of 5–6°C, in the central part between 3 and 4°C and in the southern part of Chiloé Island in a range of 4–6°C [88].

2.3. Study of the evolution of thermal zones

2.3.1. Application of Chilean regulations

In Chile, the official regulatory standard is the Thermal Regulation Application Manual (RT) [89] of the General Ordinance of Urban Planning and Construction (OGUC) [90], where seven thermal zones for building are presented based on annual values of heating degree-days with base temperature of 15°C (HDD15°C). In this context, a thermal zone is the literal translation of the Spanish term "zona térmica" which is equal to the term climatic zone for building. In Fig. 3, a map of the distribution of thermal zones in the study area is presented according to the official RT OGUC document of the year 1999, where clear coherence between the boundaries of thermal zones and the administrative division can be seen. Therefore, the RT OGUC does not consider microclimatic specifications for the study area.

Table 2 shows the intervals of the annual HDD15°C values that are used for the determination of thermal zones of RT OGUC; it also includes the values of thermal transmittance (U-values) and maximum percentage area of glazed surfaces according to RT OGUC standards that the dwellings in each thermal zone must meet.

To determine the spatial distribution of thermal zones based on meteorological data from MM5 in 360 geographical locations (Fig. 2a), the annual value of HDD15°C was calculated using the following equation [91]:

$$HDD15°C = \sum_{i=1}^{365} \left[\left(T_b - \left(\frac{T_i^{max.} + T_i^{min.}}{2} \right) \right] \right]^{+}, \quad (1)$$

where HDD is calculated as the difference between the base temperature (T_b; in this case it is 15 °C) and average daily temperature, which is calculated as half of the sum between the maximum daily temperature ($T_i^{max.}$) and the minimum daily temperature ($T_i^{min.}$); the sign (+) means that it is only necessary to calculate positive differences.

2.3.2. Data validation, scenarios and periods considered and modification of baseline climate data

Since it was decided to use the meteorological data from the 2006 MM5 model in the present research, it was necessary to show the correspondence of these model data with the data of meteorological observations. For validating meteorological data, 16 stations were selected with temperature measurements in 2006 (Fig. 4a) [92], with more than 350 days of measurements. A correlation was obtained between the annual values of the HDD15°C according to the data from meteorological stations and according to MM5 data interpolated into the coordinates of the geographical location of each station (Fig. 4b and Table 3). With a good level of correlation, generally, MM5 data are overestimated compared to data from meteorological stations. This is a logical result and is because the MM5 model data is calculated using 12.7 km grid nodes, which, because of the complexity of the relief, can be located in colder microclimatic area than meteorological stations. Also, meteorological stations can be located in the influence area of urban heat islands. Comparison of MM5 data and meteorological stations data has already been carried out for the two regions of Chile [93] and for Nicaragua [60].

Subsequently, based on MM5 data [84] in 360 geographical locations of the study area (Fig. 2a), the spatial distribution of HDD15°C was analysed and the boundaries of the thermal zones were determined in accordance with the criteria of the RT OGUC (Table 2). The MM5 meteorological data were used as baseline climate data for future calculations.

For the projections of the temperature change in the study area, data from the Center for Climate and Resilience Research (CCRR) were used [94]. For modification of the HDD15°C

values of MM5, the differences in monthly average minimum and maximum temperatures between three periods in the future and baseline climate period were used: (i) near future 2020–2035; (ii) intermediate future 2035–2050 and (iii) far future 2050–2065. In all cases, the climate change scenarios RCP2.6 and RCP8.5 available in CCRR were considered.

The differences in monthly average minimum/maximum temperatures data (Table 4), in the case of the RCP2.6 scenario, were based on the average simulation results of 22 global models, 4 regional models and 2 local models. The RCP8.5 scenario has been based on the average simulation results of 35 global models of the Coupled Model Intercomparison Project (CMIP5) [95], 7 regional climate models and 2 local models [94].

In addition, it is necessary to analyse the projections of changing temperatures in the research area. In Fig. 5, the intra-annual variability of the expected differences in monthly average minimum/maximum temperatures for the entire study area can be observed. It can be seen that, for both temperatures, there is a variability of expected temperature changes with maximum in the summer months and minimum in the winter months. This variability is clear in all future periods and for both scenarios. On the other hand, for the monthly average maximum expected temperature, the changes are higher (Fig. 5b) than for the monthly average minimum temperature (Fig. 5a). This phenomenon can be connected with the maximum temperature being a more sensitive meteorological parameter and reflects changes in the synoptic regime and changes in daytime radiative balance in the future.

A similar conclusion can be traced from an analysis of Fig. 6, which presents box-plots of the variability of the expected differences in annual average minimum (Fig. 6a) and maximum (Fig. 6b) temperatures in the 360 geographical locations of the study area. Also, it can be seen that for the RCP2.6 scenario, a stabilisation of change is observed after the 2035–2050 period in both temperatures, so the variability of the expected temperature change is quite similar in the periods 2050–2065 and 2035–2050, which is consistent with the main geophysical idea of the RCP2.6 scenario.

Additionally, in Fig. 7, the spatial distribution maps of the differences in annual average temperature (average between maximum and minimum temperature and between the two scenarios RCP2.6 and RCP 8.5) are presented for three periods in the future as compared to the baseline climate. It can be seen that the average annual temperature change for the entire study area is generally positive for the three periods, however, it is not spatially homogeneous. The maximum temperature rise is expected in the mountainous area of the northeast. A minimum temperature increase, for all periods in the future, is observed for the coast south of the city of Valdivia. For the period 2020–2035, an annual average temperature increase between +0.45 to +0.65 °C is expected; for the period 2035–2050 this interval is between +0.65 to +0.95 °C and for the period 2050–2065 the temperature increase will range between +0.95 to +1.25 °C as compared to baseline climate.

Intra-annual and spatial heterogeneity of the expected changes in the minimum and maximum temperature in the study area observed was based on data from a large number of climatic models. Therefore, these data can be applied to change baseline climate data and analyse changes in future thermal zone scenarios.

The modification of daily temperature data of MM5 will be carried out in accordance with methodologies already presented in other scientific works [31,96,97]. Based on Jiang A. et al. and Belcher S.E. et al. [96,97], it is possible to apply “a shift” algorithm to modify the baseline climate data to edit the daily values of maximum and minimum baseline climate temperatures by adding the projected monthly average difference for future periods. This methodology has uncertainties that should be noted:

- first, the quality of data in future periods depends primarily on the quality of data in the baseline climate period. The reliability level of the MM5 data was noted previously.

- second, the quality of data in the future depends on the quality of climate modelling for future climate change scenarios. Therefore, data on the average results of the ensemble of climate models were used in this work to reduce inaccuracies in reproducing the future temperature of some climate models in the study area.

Based on this, the calculation of HDD15°C values in the future will be done by applying the following equation:

$$HDD\ 15°C_f = \sum_{j=1}^{12}\sum_{i=1}^{k}\left[(T_b - \left(\frac{(T_i^{max.}+\Delta_j^{max.})+(T_i^{min.}+\Delta_j^{min.})}{2}\right)\right]^+, \quad (2)$$

where T_b – base temperature (15°C); $T_i^{max.}$ – maximum daily temperature of MM5 in baseline climate period; $T_i^{min.}$ – minimum daily temperature of MM5 in baseline climate period; $\Delta_j^{max.}/\Delta_j^{min.}$ – differences in monthly average maximum/minimum temperatures between future periods (2020–2035; 2035–2050; 2050–2065) and the baseline climate; k – number days in each month and the sign (+) means that it is only necessary to calculate positive differences. Values of $\Delta_j^{max.}$ and $\Delta_j^{min.}$ were taken from the website of CCRR [94]. For scenarios RCP2.6 and RCP 8.5, $\Delta_j^{max.}$ and $\Delta_j^{min.}$ are average values of 28 and 44 climate models, respectively (Table 4). Therefore, to modify the daily data on the maximum and minimum temperatures of the baseline climate in each geographical location (Fig. 2a), a data set was created with 36 values of $\Delta_j^{max.}$ and 36 of values $\Delta_j^{min.}$ for each geographical point and for each scenario of climate change. The Kriging interpolation method is used to restore the spatial distribution of all parameters [98].

2.4. Simulation of heating energy consumption

2.4.1. Description of dwelling type

To carry out the energy simulation, a dwelling of the real estate type was used, with a 76.20 m^2 constructed area and a 66.37 m^{2}useful area. This is a typical type of house in the southern part of Chile. This is an existing house with two inhabitants, and it is in the city of Valdivia. Geographic coordinates of the area where the house is located are - 39°47´58´´S 73°12´30´´W. Architectural plans and a three-dimensional view are shown in Fig. 8. The housing stock in Chile is 6.5 million dwellings. The number of houses and apartments represent 79.9% and 17.5% of the existing residential building stock, respectively [99,100]. According to Molina C. et al. [100], the average floor area for dwellings in Chile is 66 m^2 and two-story houses with a 64–79 m^2 area represent 14.4% of the total housing stock of the country.

Table 5 shows the thermal transmittance of the different construction elements of a house used for 3-D modelling and energy simulation. The dwelling roof and walls meet the standards for thermal zone 6, other construction elements comply with the regulations for the colder thermal zone, zone 7.

To simulate heating EC HVAC system “Residential 14 SEER/8.3 HSPF Split/Packaged Heat Pump” from the Revit standard library was used. This system was an efficient < 5.5-ton split/packaged heat pump system with 8.3 Heating Seasonal Performance Factor and 14 Seasonal Energy Efficiency Ratio for cooling. According to references [101,102], the seasonal COP value for heating of this system is 2.43, and seasonal COP for cooling is 4.10. This HVAC system includes other elements: (i) Residential constant volume cycling fan; (ii) 2.0 inch of water gauge (498 pascals) static pressure constant volume duct system; (iii)

Integrated differential dry-bulb temperature economizer [103]. The heating part of this system is electrical, and values of the EC are presented in kWh.

EC simulation was carried out for 8760 hours over a calendar year in 360 geographical locations of the study area (Fig. 2a). In all areas of the house, heating was simulated to 20°C. According to the Sustainable Construction Standards for building in Chile of the Ministry of Housing and Urban Development of Chile [104], from the minimum values for the intervals of internal thermal comfort in the thermal zones of the country—where heating is necessary—20°C is the maximum value accepted.

Occupation by two persons was considered for the simulation. Currently, in European countries such as Denmark and the United Kingdom, the average household size is 2.1 [105] and 2.48 [100] people per house, respectively. In South America, in Chile and in Colombia, the average household size is 3.64 [100] and 3.9 [105] people per house, respectively. However, according to forecasts, by 2100 in Colombia, the average household size will decrease to 2.09–2.85 people per house, depending on the forecast of the country's economic development [105]. Based on these projections, it was decided to leave the occupation of the house with two people for simulation. Subsequently, the results of an EC simulation will be projected into the future.

Additional simulation parameters, such as sensible heat gains per person – 73.27 W and latent heat gains per person - 45.43 W, were taken from the standard Revit library for residential dwellings. These values are close to the values presented in other studies. So, for example, in the work of Martin M. et al. [106], to simulate the EC of a residential dwelling, the authors used – 70 W for the value of sensible heat gains per person and - 50 W for latent heat gains per person. In Moreno A. et al. [107], the authors used - 80 W for the value of sensible heat gains per person and 40 W for latent heat gains per person. The method used to calculate outdoor airflow to space depends on dwellers and useful surface area. Outdoor air per person was 2.36 L/s and outdoor air per area was 0.30 L/s·m^2. Fig. 9 shows the occupancy schedule settings applied in the energy simulation. These settings are from the Revit standard library for residential buildings. For hourly simulations, parameters that affect EC of a dwelling and are dependent on the people present will be multiplied by a factor shown in Fig. 9.

In the present research, only the results of heating EC simulation were considered. The regions under study are characterized by a high-level of wood use for heating dwellings. Government programs are aimed at reducing heating EC and also at reducing the environmental and epidemiological consequences for the population of these regions [65]. Therefore, the present work will help to detail geographical areas with a high level of heating EC and evaluate the natural potential of reducing heating EC in the context of climate change. Currently, in the study area, there is no problem related to the cooling EC of dwellings. But in the future, it will also be important to evaluate changes in cooling EC.

2.4.2. Estimation of heating energy consumption in the future

For the estimation of heating EC for the future, the quotient between heating EC and HDD15°C of baseline climate will be used, which demonstrates the amount of energy for heating (kWh/m^2/year) corresponding to a degree-day of heating with a base of 15 °C in each geographical location. This will reveal geographic regions with the same annual value of HDD15°C, but with different EC values. Thus, assuming that the quotient between heating EC and HDD15°C will be maintained in different geographical areas in the future, the future heating EC can be calculated in a first approximation, which will depend only on temperature

changes in conditions of global climate change expected in the study area. The heating EC value expected in the future (EC_f) will be calculated with the equation:

$$EC_f = \frac{EC_a}{HDD15°C} \cdot HDD15°C_f \quad (3)$$

where EC_a— heating EC according to the simulation results in GBS, $HDD15°C$ – value obtained from Eq. 1 of baseline climate; $HDD15°C_f$ – HDD15°C value in future period, calculated according to Eq. 2. Currently, in the scientific literature there have been no studies that consider a similar methodology and that have used the quotient between heating EC and HDD as a parameter that can be implemented to estimate changes EC and climate zoning for building in a fairly large geographical area.

3. Results and discussion

In order to know the effects that climate change will have on heating EC in the study area, the situation of the thermal zones distribution in the baseline climate period was analysed first, as well as the foreseeable changes; subsequently, the EC in the baseline climate period will be simulated and finally estimated for the future.

3.1. Thermal zones distribution

3.1.1. Thermal zones in baseline climate period

In accordance with the provisions of the official RT OGUC document for the study area, four thermal zones are presented (4, 5, 6 and 7). In Fig. 3 and in Table 6 (column "Of. Doc. RT OGUC 1999"), these zones are represented and the results of thermal zones of the official document for each principality of the communes are collected. It can be seen that most of the cities belong to thermal zones 5 and 6; specifically, out of the 74 cities listed in Table 6, 37 are in zone 5 and 31 in zone 6. And six cities located in small areas in the northwest and southeast belong to thermal zone 4 (four cities) and thermal zone 7 (two cities), respectively.

If the spatial distribution of HDD15°C of the MM5 data for the year 2006 is analysed (Fig. 10a), it is observed that its annual values range between 1000 and 4000, with maximum values in the southeast part in mountainous areas, and minimum values west of Temuco city and along the shore of the inner bay, located south of Puerto Montt city. Based on these values, and with the thermal zoning recommendations of RT OGUC (Table 2), the baseline climate thermal zones presented in Fig. 10b have been restored. If a comparison is made with the distribution of the thermal zones of the official RT OGUC document (Fig. 3), a notable difference is observed; for example, the entire area of mountains on the east is characterised by belonging to thermal zone 7 as compared to zone 6 which is specified in the current RT OGUC document. Also, the area within thermal zone 4 is smaller as compared with RT OGUC. Table 6 (column “MM5 baseline climate 2006”) shows the thermal zones for each city with annual values of HHD15°C. Cities like Valdivia and Temuco are located in thermal zone 5, while Puerto Montt is located between thermal zones 5 and 6. In comparison, according to the official document of RT OGUC, Puerto Montt city is located in thermal zone 6. Another notable difference is that 11 cities are located in thermal zone 7. It should be noted that the official RT OGUC document defines a warmer thermal zone in cities where a colder thermal zone is observed by MM5 data. This difference is noticed thanks to the high spatial resolution of MM5 data, which reflects more microclimatic specifications in the study area.

The differences found are explained because the thermal zones of the official RT OGUC document are based on administrative boundaries, so they do not reflect the microclimatic diversity of the region under study, which is why this standard has already been criticised [108,109]; nevertheless, they have not been updated in a long period [65].

In the research [65] also determined the boundaries of thermal zones for a similar geographical area. However, the data was only from 35 meteorological stations over the past decade. The methodology for determining the thermal zones boundaries was manual-cartographic. The border refinement was based on bioclimatic maps and the official RT OGUC map. Therefore, for example, in the Andes region on the border with Argentina, it was not possible to clearly establish the boundaries of thermal zone 7, which was performed in present work. In addition, not all meteorological stations had a sufficient set of meteorological data, which are necessary to simulate EC. Additionally, MM5 data is from 2006, but with their detailed spatial resolution, this data reflects the microclimatic features of the studied area. Therefore, the boundaries of the zones obtained in the present study do not coincide with the previous work. MM5 data makes it possible to carry out multiple simulations, mapping and analysis of the spatial distribution of EC [93]. Also, MM5 data can potentially be used to modify meteorological data files used for simulation in other tools, for example, in Energy Plus [60].

3.1.2. Forecast evolution of the thermal zones

In Fig. 11, the RT OGUC thermal zone maps are recalculated based on baseline climate data and taking into account thermal effects (temperature changes only) of climate change in the study area (section 2.3.2). In Table 6, numbers of RT OGUC thermal zones and HDD15°C values of baseline climate for principal cities are presented for three future periods, 2020–2035, 2035–2050 and 2050–2065, and for the two scenarios of climate change: RCP2.6 and RCP8.5. As has happened in other studies, a change in climatic zones to warmer ones can be observed [47]. For the baseline climate period in cities in the Araucanía region, the HDD15°C values are in the range 1025–3021; in the Los Ríos region 1395–1864 and in the Los Lagos region 1187–3940. The average decrease in these values for the 2050–2065 period in the entire study area will be 12% and 27% for the RCP2.6 and RCP8.5 scenarios, respectively, that is, the changes will be more drastic in the case of the second scenario.

In the case of scenario RCP2.6 (Fig. 11c, e), the main changes in thermal zones will happen until the period 2035–2050. Because this climate change scenario predicts that the climate will stabilise and decelerate in subsequent periods [6]. As a consequence of climate change, in the northwest part of the study area, in the period 2020–2035 (Fig. 11a) thermal zone 3 begins to form, specifically to the west of Temuco city. On the other hand, the borders of thermal zone 7 will not vary much. For the period 2050–2065 and scenario RCP2.6, six cities will be located in thermal zone 7; 11 cities will be located in thermal zone 6; 25 cities in thermal zone 5; 31 cities in thermal zone 4 and one city will be located in thermal zone 3. In total 50 out of 74 cities in the 2050–2065 period will experience changes in thermal zones from baseline climate to a warmer zone (Table 6).

More drastic changes are observed for scenario RCP8.5, especially in the period 2050–2065 in which thermal zone 2 in the northwest part (Fig. 11f), specifically in the city of Puerto Saavedra (Table 6) and in the part of Chiloé Island (southwest Fig. 11d) will change as thermal zone 3 begins to form in the period 2035–2050 (Table 6, Curaco de Vélez city). For the period 2050–2065 and scenario RCP8.5, six cities will be located in thermal zone 7; 5 cities will be located in thermal zone 6; 8 cities in thermal zone 5; 31 cities in thermal zone 4; 23 cities in thermal zone 3 and 1 city will be located in thermal zone 2 (Table 6). For 37 cities, the baseline climate thermal zones will change by two thermal zones and 31 cities will change their zones for one warmer, 6 cities will remain unchanged; this will happen in cities located in mountainous areas with thermal zone 7.

After comparison of predicted thermal zones with baseline climate thermal zones, we proceeded to analyse the application of current RT OGUC standards to the future and comparison of the thermal zones presented in the RT OGUC with the predicted thermal zones. It can be seen (Table 7) that, in 2020–2035, thermal zones are preserved by 47% (RCP2.6) and in 38% (RCP8.5) of cities. Warmer thermal zones will be observed in 35% (RCP2.6) and 47% (RCP8.5) of cities. For the next period (2035–2050), the number of cities with preserved thermal zones will decrease to 36.5% (RCP2.6) and 28% (RCP8.5). In parallel, the number of cities where thermal zones will change to warmer will increase up to 50% (RCP2.6) and up to 61% (RCP8.5). In the period 2050–2065, only 35% and 15% of the cities will maintain their thermal zone with respect to scenarios RCP2.6 and RCP8.5, respectively. In 13.5% (RCP2.6) and 8% (RCP8.5) of the cities under study, it is necessary to improve the housing insulation regulations, since in those cities, a colder climate is actually observed compared to the information proposed by the official RT OGUC document. For other cities, 51.5% (RCP2.6) and 77% (RCP8.5) need to adapt the current RT OGUC regulations to climate change in order to optimise the housing construction and operating costs for future warmer weather conditions. In any situation, with a scenario of stabilisation of climate change (RCP2.6) and a scenario of drastic climate change (RCP8.5), considerable changes in thermal zones are observed. For this reason, the current RT OGUC construction regulations must be updated, improved and adapted to future climatic changes in the study area.

3.2. Heating energy consumption

3.2.1. Heating energy consumption in baseline climate period

The heating EC has been simulated in the baseline climate period, which allowed us to obtain the results shown in Fig. 12, in which the structure of the heating EC isolines is similar to the HDD15°C isolines shown in Fig. 10a. The variability of heating EC and HDD15°C is in a range of 60–300 kWh/m^2/year and 1000–4000, respectively. This is a consequence of the MM5 meteorological data used for energy simulation. The average value of heating EC observed for all cities is 106 kWh/m^2/year (σ = 37kWh/m^2/year) with a maximum in the case of dwellings located in the mountainous part, generally in the southeast part of the study area (250–300kWh/m^2/year), and a minimum value that is reached on the northwest oceanic coast (60kWh/m^2/year). Specifically in Table 8, results of simulation of heating EC in the cities are presented, in which Futaleufú, a city in the southeast of the study area, has the highest heating EC value of 286 kWh/m^2/year, while the minimum of 65 kWh/m^2/y was observed in Puerto Saavedra, located in the northwestern part.

If the heating EC is related to the annual HDD15°C values in all the energy simulation points of the study area (Fig. 13), a linear correlation between these two parameters can be observed, similar to the work of Conradie et al. [110]. On the other hand, there is also a sufficient data difference; thus, for the value of HDD15°C equal to 3,000, it can be seen that the heating EC can range between 175 kWh/m^2/year and 225 kWh/m^2/year. This means that different geographical locations with the same annual HDD15°C value will have different heating EC values, and this difference can be explained by the fact that the energy simulation is carried out on the basis of different hourly meteorological parameters in every geographic place [93], and the HDD15°C values were calculated by the maximum and minimum daily temperatures. Due to this correlation, it can be established that in each geographical location there is a conversion coefficient between HDD15°C and heating EC, so for each geographical point of energy simulation it has been possible to calculate the quotient between heating EC

and HDD15°C for the baseline climate period. In Fig. 14, the spatial distribution map of the quotient between heating EC and HDD15°C for 2006 is shown.

It can be seen, that in high-altitude mountain areas, a quotient greater than 0.070kWh/m^2/year per HDD15°C is observed, while, in the southern part, near Puerto Montt, this quotient is at the threshold of 0.050–0.055 kWh/m^2/year per HDD15°C. Similarly, near large lakes, there are areas with a minimum quotient between heating EC and HDD15°C. Thus, Mourshed M. [32] describes the coefficient between HDD and heating EC as dependent on the overall seasonal heating system efficiency and the overall building heat loss coefficient. Therefore, for a single house with the same operating conditions, the same heating system, the same orientation with respect to north and other similar characteristics, variability of heating EC in two different geographical locations with the same value of HDD15°C, will generally depend on heat loss. Which will, in turn, depend on other meteorological parameters, mainly wind (speed and direction will affect infiltration of air) and solar radiation (will affect external heat gain).

It can therefore be concluded that the quotient between heating EC and HDD15°C can be used as a quantitative characteristic of some areas with similar climatic conditions, where a linear relationship between heating EC and HDD15°C is observed. Of course, each house, with its own characteristics of architecture, construction and other individual parameters, will have different absolute values of the quotient between heating EC and HDD15°C; but the spatial distribution of this quotient with its zones of maximum and minimum will be maintained. For all this, the use of the energy simulation results together with HDD data will help with climatic zoning for building in areas with cold climates.

3.2.2. Forecast change of heating energy consumption

Finally, heating EC of the dwelling under study has been estimated for the future, taking into account the two climate change scenarios and the three periods considered. The results are presented in Fig. 15. Since the estimation of heating EC has been based solely on HDD changes for the study area, it can be said that this heating EC takes into account only future temperature changes.

If Fig. 15 is compared with Fig. 12, it is observed that the isolines shape and spatial distribution of EC for heating are similar. Thus, in the period 2020–2035, the EC for heating will decrease (on average between the two scenarios RCP2.6 and RCP8.5) between 5 kWh/m^2/year and 20 kWh/m^2/year. In the period 2050–2065 the reduction will be greater, estimated between 10 kWh/m^2/year and 25 kWh/m^2/year; and finally, in period 2050–2065, it will reach values between 12 kWh/m^2/year and up to 45 kWh/m^2/year.

Table 8 shows the estimating heating EC of the dwelling under study in principal cities in the southern part of Chile for the period 2050–2065. It can be seen that the heating EC values will have a decreasing trend in all cities and for the two scenarios analysed. However, this does not mean that a decrease in heating EC is a positive effect for reduce of total EC, because can increase part of the consumption for cooling and ventilation of the houses [58].

The decreases calculated between 2006 and 2050–2065 for scenario RCP2.6 are 13%, with an average value of heating EC of 94 kWh/m^2/year (σ = 36kWh/m^2/year). In the case of the most extreme RCP8.5 scenario, this decrease would be 27% with an average heating EC value of 79 kWh/m^2/year (σ= 34kWh/m^2/year).

Similar results have been observed in cities of the southern hemisphere. For example, Wang et al. [35] estimated for the city of Hobart, located at the southern tip of Tasmania Island (42.9°S), that the heating EC of residential dwellings will decrease of 25% (42%) and

28% (58%) in the year 2050 (2100), under the A1B and A1FI scenarios, respectively. Flores-Larsen et al. [42] analysed the change in EC in four cities in Argentina located between latitudes 23°S–37°S under the SRES A2 scenario, concluding that, by the year 2080 in an isolated single-family home, the heating EC will decrease in the range of 23–59%. The minor changes in the heating EC observed in our research, for scenario RCP2.6, are due to the fact that this climate change mitigation scenario is the most positive for the world with minimisation of anthropogenic effects to climate system.

Finally, differences are observed between mountain and coastal areas. Thus, for the period 2050–2065 and RCP8.5, in Lonquimay city, the decrease in heating EC of 42 kWh/m^2/year is observed in absolute values (corresponding to only 19% of the consumption in 2006). On the other hand, the coastal city of Dalcahue, on Chiloe Island, shows a decrease in heating EC for 23 kWh/m^2/year in absolute values (corresponding to 29% of consumption in 2006), not being as significant as in the mountainous area.

4. Conclusions

The main conclusions derived from the present investigation have been the following:

- From the point of view of the current situation and taking into account the results obtained for the "baseline climate," the official document RT OGUC is shown to be inconsistent with the study area climatological reality because it establishes the thermal zones as a function of administrative boundaries, not climatic ones. This means that today its application would imply a building design that does not agree with the temperatures in which it is located. This problem will get worse in most cities in the future.
- As for the expected temperature changes, these are positive throughout the study area and provide trends of decrease of HDD°15 in the entire investigated zone.
- The simulation results of the heating EC of a single-family house for the baseline climate period showed five-fold variability, between 60kWh/m^2/year and 300kWh/m^2/year due to the diversity of microclimatic zones within the study area.
- The methodology for estimating heating EC for the future has been demonstrated, taking into account the effect of temperature change in the future and the quotient between heating EC and HDD of baseline climate. In addition, discussions were held on the possibility of applying this quotient in the improvement of climatic zoning for building. This methodology can be implemented in other regions of the world.
- As a consequence of the variation of the thermal zones, we expected a decrease of the heating EC of 5–15%, 6–24%, 7–34% (under the two scenarios RCP 2.6 and RCP 8.5) for future periods 2020–2035, 2035–2050 and 2050–2065, respectively. Given that the changes in total EC depend not only on the consumption for heating, but also on the need for cooling and ventilation of the house, the need to extend this study in their determination is evident.
- The method of energy simulation in numerous geographical locations with different types of dwellings, the matching of energy results with weather parameters and adaptation and mitigation methods for climate change are priorities for the development of the correct climatic zone determination for building in the future.

Acknowledgements

This research was supported by the Comisión Nacional de Investigación Científica y Tecnológica (CONICYT) (National Commission for Scientific and Technological Research) of Chile, through the Fondo Nacional de Desarrollo Científico y Tecnológico

(FONDECYT) (National Fund for Scientific and Technological Development) with the projects CONICYT FONDECYT 11160524; CONICYT FONDECYT 1201052; CONICYT PFCHA/DOCTORADO BECAS CHILE/2019 – 21191227; Vicerrectoría de Investigación (VRI) (Vice-Rectory of Research) of the Pontificia Universidad Católica de Chile, through the Concurso Pasantías y Estadías Breves de Investigación Convocatoria 2019 (Internship and Short Research Stays Contest - Call 2019) PEBI1909; and research group TEP-968 Tecnologías para la Economía Circular (Technologies for Circular Economy) of the University of Granada, Spain.

References

[1] IPCC, Climate Change 2013: The Physical Science Basis. Contribution of Working Group I to the Fifth Assessment Report of the Intergovernmental Panel on Climate Change, Cambridge University Press, Cambridge, United Kingdom and New York, NY, USA, 2013.

[2] IPCC, Emissions Scenarios, Cambridge, 2000.

[3] IPCC, IPCC, 2001: Climate Change 2001: The Scientific Basis. Contribution of Working Group I to the Third Assessment Report of the Intergovernmental Panel on Climate Change, Cambridge University Press, Cambridge, United Kingdom and New York, NY, USA, 2001.

[4] IPCC, Climate Change 2007: The Physical Science Basis, Contribution of Working Group I to the Fourth Assessment Report of the Intergovernmental Panel on Climate Change, Cambridge University Press, 2007.

[5] D.P. Van Vuuren, M.G.J. Den Elzen, P.L. Lucas, B. Eickhout, B.J. Strengers, B. Van Ruijven, S. Wonink, R. Van Houdt, Stabilizing greenhouse gas concentrations at low levels: An assessment of reduction strategies and costs, Clim. Change. 81 (2007) 119–159. doi:10.1007/s10584-006-9172-9.

[6] D.P. Van Vuuren, E. Stehfest, M.G.J. den Elzen, T. Kram, J. van Vliet, S. Deetman, M. Isaac, K.K. Goldewijk, A. Hof, A.M. Beltran, R. Oostenrijk, B. van Ruijven, RCP2.6: Exploring the possibility to keep global mean temperature increase below 2°C, Clim. Change. 109 (2011) 95–116. doi:10.1007/s10584-011-0152-3.

[7] A.M. Thomson, K. V. Calvin, S.J. Smith, G.P. Kyle, A. Volke, P. Patel, S. Delgado-Arias, B. Bond-Lamberty, M.A. Wise, L.E. Clarke, J.A. Edmonds, RCP4.5: A pathway for stabilization of radiative forcing by 2100, Clim. Change. 109 (2011) 77–94. doi:10.1007/s10584-011-0151-4.

[8] T. Masui, K. Matsumoto, Y. Hijioka, T. Kinoshita, T. Nozawa, S. Ishiwatari, E. Kato, P.R. Shukla, Y. Yamagata, M. Kainuma, An emission pathway for stabilization at 6 Wm-2radiative forcing, Clim. Change. 109 (2011) 59–76. doi:10.1007/s10584-011-0150-5.

[9] K. Riahi, S. Rao, V. Krey, C. Cho, V. Chirkov, G. Fischer, G. Kindermann, N. Nakicenovic, P. Rafaj, RCP 8.5-A scenario of comparatively high greenhouse gas emissions, Clim. Change. 109 (2011) 33–57. doi:10.1007/s10584-011-0149-y.

[10] M. Olonscheck, A. Holsten, J.P. Kropp, Heating and cooling energy demand and related emissions of the German residential building stock under climate change, Energy Policy. 39 (2011) 4795–4806. doi:https://doi.org/10.1016/j.enpol.2011.06.041.

[11] D.A. Asimakopoulos, M. Santamouris, I. Farrou, M. Laskari, M. Saliari, G. Zanis, G. Giannakidis, K. Tigas, J. Kapsomenakis, C. Douvis, S.C. Zerefos, T. Antonakaki, C. Giannakopoulos, Modelling the energy demand projection of the building sector in

Greece in the 21st century, Energy Build. 49 (2012) 488–498. doi:https://doi.org/10.1016/j.enbuild.2012.02.043.

[12] P. Xu, Y.J. Huang, N. Miller, N. Schlegel, P. Shen, Impacts of climate change on building heating and cooling energy patterns in California, Energy. 44 (2012) 792–804. doi:https://doi.org/10.1016/j.energy.2012.05.013.

[13] J.A. Dirks, W.J. Gorrissen, J.H. Hathaway, D.C. Skorski, M.J. Scott, T.C. Pulsipher, M. Huang, Y. Liu, J.S. Rice, Impacts of climate change on energy consumption and peak demand in buildings: A detailed regional approach, Energy. 79 (2015) 20–32. doi:https://doi.org/10.1016/j.energy.2014.08.081.

[14] R. Aguiar, M. Oliveira, H. Gonccedilalves, Climate change impacts on the thermal performance of Portuguese buildings. Results of the SIAM study, Build. Serv. Eng. Res. Technol. 23 (2002) 223–231. doi:10.1191/0143624402bt045oa.

[15] T. Frank, Climate change impacts on building heating and cooling energy demand in Switzerland, Energy Build. 37 (2005) 1175–1185. doi:https://doi.org/10.1016/j.enbuild.2005.06.019.

[16] M.R. Gaterell, M.E. McEvoy, The impact of climate change uncertainties on the performance of energy efficiency measures applied to dwellings, Energy Build. 37 (2005) 982–995. doi:https://doi.org/10.1016/j.enbuild.2004.12.015.

[17] M. Dolinar, B. Vidrih, L. Kajfež-Bogataj, S. Medved, Predicted changes in energy demands for heating and cooling due to climate change, Phys. Chem. Earth, Parts A/B/C. 35 (2010) 100–106. doi:https://doi.org/10.1016/j.pce.2010.03.003.

[18] Z. Ren, Z. Chen, X. Wang, Climate change adaptation pathways for Australian residential buildings, Build. Environ. 46 (2011) 2398–2412. doi:https://doi.org/10.1016/j.buildenv.2011.05.022.

[19] C. Kendrick, R. Ogden, X. Wang, B. Baiche, Thermal mass in new build UK housing: A comparison of structural systems in a future weather scenario, Energy Build. 48 (2012) 40–49. doi:https://doi.org/10.1016/j.enbuild.2012.01.009.

[20] R. Gupta, M. Gregg, Using UK climate change projections to adapt existing English homes for a warming climate, Build. Environ. 55 (2012) 20–42. doi:https://doi.org/10.1016/j.buildenv.2012.01.014.

[21] J.N. Hacker, T.P. De Saulles, A.J. Minson, M.J. Holmes, Embodied and operational carbon dioxide emissions from housing: A case study on the effects of thermal mass and climate change, Energy Build. 40 (2008) 375–384. doi:https://doi.org/10.1016/j.enbuild.2007.03.005.

[22] A. Mavrogianni, P. Wilkinson, M. Davies, P. Biddulph, E. Oikonomou, Building characteristics as determinants of propensity to high indoor summer temperatures in London dwellings, Build. Environ. 55 (2012) 117–130. doi:https://doi.org/10.1016/j.buildenv.2011.12.003.

[23] M. Barclay, S. Sharples, J. Kang, R. Watkins, The natural ventilation performance of buildings under alternative future weather projections, Build. Serv. Eng. Res. Technol. 33 (2011) 35–50. doi:10.1177/0143624411427460.

[24] S. Shikder, M. Mourshed, A. Price, Summertime impact of climate change on multi-occupancy British dwellings, Open House Int. 37 (2012) 50–60. https://www.scopus.com/inward/record.uri?eid=2-s2.0-84872941611&partnerID=40&md5=909648e5f1b47631674b1867f172b1f1.

[25] S.M. Sajjadian, J. Lewis, S. Sharples, The potential of phase change materials to reduce domestic cooling energy loads for current and future UK climates, Energy

Build. 93 (2015) 83–89. doi:https://doi.org/10.1016/j.enbuild.2015.02.029.
[26] M. Hamdy, S. Carlucci, P.-J. Hoes, J.L.M. Hensen, The impact of climate change on the overheating risk in dwellings—A Dutch case study, Build. Environ. 122 (2017) 307–323. doi:https://doi.org/10.1016/j.buildenv.2017.06.031.
[27] H. Radhi, Evaluating the potential impact of global warming on the UAE residential buildings – A contribution to reduce the CO2 emissions, Build. Environ. 44 (2009) 2451–2462. doi:10.1016/J.BUILDENV.2009.04.006.
[28] H. Kikumoto, R. Ooka, Y. Arima, T. Yamanaka, Study on the future weather data considering the global and local climate change for building energy simulation, Sustain. Cities Soc. 14 (2015) 404–413. doi:https://doi.org/10.1016/j.scs.2014.08.007.
[29] Y. Arima, R. Ooka, H. Kikumoto, T. Yamanaka, Effect of climate change on building cooling loads in Tokyo in the summers of the 2030s using dynamically downscaled GCM data, Energy Build. 114 (2016) 123–129. doi:https://doi.org/10.1016/j.enbuild.2015.08.019.
[30] K. Jylhä, J. Jokisalo, K. Ruosteenoja, K. Pilli-Sihvola, T. Kalamees, T. Seitola, H.M. Mäkelä, R. Hyvönen, M. Laapas, A. Drebs, Energy demand for the heating and cooling of residential houses in Finland in a changing climate, Energy Build. 99 (2015) 104–116. doi:https://doi.org/10.1016/j.enbuild.2015.04.001.
[31] A.L.S. Chan, Developing future hourly weather files for studying the impact of climate change on building energy performance in Hong Kong, Energy Build. 43 (2011) 2860–2868. doi:https://doi.org/10.1016/j.enbuild.2011.07.003.
[32] M. Mourshed, The impact of the projected changes in temperature on heating and cooling requirements in buildings in Dhaka, Bangladesh, Appl. Energy. 88 (2011) 3737–3746. doi:https://doi.org/10.1016/j.apenergy.2011.05.024.
[33] Y. Yildiz, Analysis of Performance of Night Ventilation for Residential Buildings in Hot-Humid Climates, J. Fac. Eng. Archit. Gazi Univ. 29 (2014) 385–393.
[34] K.-T. Huang, R.-L. Hwang, Future trends of residential building cooling energy and passive adaptation measures to counteract climate change: The case of Taiwan, Appl. Energy. 184 (2016) 1230–1240. doi:https://doi.org/10.1016/j.apenergy.2015.11.008.
[35] X. Wang, D. Chen, Z. Ren, Assessment of climate change impact on residential building heating and cooling energy requirement in Australia, Build. Environ. 45 (2010) 1663–1682. doi:https://doi.org/10.1016/j.buildenv.2010.01.022.
[36] A. Invidiata, E. Ghisi, Impact of climate change on heating and cooling energy demand in houses in Brazil, Energy Build. 130 (2016) 20–32. doi:https://doi.org/10.1016/j.enbuild.2016.07.067.
[37] M.A. Triana, R. Lamberts, P. Sassi, Should we consider climate change for Brazilian social housing? Assessment of energy efficiency adaptation measures, Energy Build. 158 (2018) 1379–1392. doi:https://doi.org/10.1016/j.enbuild.2017.11.003.
[38] H. Wang, Q. Chen, Impact of climate change heating and cooling energy use in buildings in the United States, Energy Build. 82 (2014) 428–436. doi:https://doi.org/10.1016/j.enbuild.2014.07.034.
[39] P. Shen, N. Lior, Vulnerability to climate change impacts of present renewable energy systems designed for achieving net-zero energy buildings, Energy. 114 (2016) 1288–1305. doi:https://doi.org/10.1016/j.energy.2016.07.078.
[40] P. Shen, Impacts of climate change on U.S. building energy use by using downscaled hourly future weather data, Energy Build. 134 (2017) 61–70. doi:https://doi.org/10.1016/j.enbuild.2016.09.028.

[41] A. Robert, M. Kummert, Designing net-zero energy buildings for the future climate, not for the past, Build. Environ. 55 (2012) 150–158. doi:https://doi.org/10.1016/j.buildenv.2011.12.014.
[42] S. Flores-Larsen, C. Filippín, G. Barea, Impact of climate change on energy use and bioclimatic design of residential buildings in the 21st century in Argentina, Energy Build. 184 (2019) 216–229. doi:https://doi.org/10.1016/j.enbuild.2018.12.015.
[43] A. Dodoo, L. Gustavsson, F. Bonakdar, Effects of Future Climate Change Scenarios on Overheating Risk and Primary Energy Use for Swedish Residential Buildings, Energy Procedia. 61 (2014) 1179–1182. doi:https://doi.org/10.1016/j.egypro.2014.11.1048.
[44] C. Roux, P. Schalbart, E. Assoumou, B. Peuportier, Integrating climate change and energy mix scenarios in LCA of buildings and districts, Appl. Energy. 184 (2016) 619–629. doi:https://doi.org/10.1016/j.apenergy.2016.10.043.
[45] I. Andrić, N. Gomes, A. Pina, P. Ferrão, J. Fournier, B. Lacarrière, O. Le Corre, Modeling the long-term effect of climate change on building heat demand: Case study on a district level, Energy Build. 126 (2016) 77–93. doi:https://doi.org/10.1016/j.enbuild.2016.04.082.
[46] C.A. Alves, D.H.S. Duarte, F.L.T. Gonçalves, Residential buildings' thermal performance and comfort for the elderly under climate changes context in the city of São Paulo, Brazil, Energy Build. 114 (2016) 62–71. doi:https://doi.org/10.1016/j.enbuild.2015.06.044.
[47] Z.J. Zhai, J.M. Helman, Implications of climate changes to building energy and design, Sustain. Cities Soc. 44 (2019) 511–519. doi:https://doi.org/10.1016/j.scs.2018.10.043.
[48] D.J. Sailor, Risks of summertime extreme thermal conditions in buildings as a result of climate change and exacerbation of urban heat islands, Build. Environ. 78 (2014) 81–88. doi:https://doi.org/10.1016/j.buildenv.2014.04.012.
[49] L. Pierangioli, G. Cellai, R. Ferrise, G. Trombi, M. Bindi, Effectiveness of passive measures against climate change: Case studies in Central Italy, Build. Simul. 10 (2017) 459–479. doi:10.1007/s12273-016-0346-8.
[50] C. Filippín, F. Ricard, S. Flores Larsen, M. Santamouris, Retrospective analysis of the energy consumption of single-family dwellings in central Argentina. Retrofitting and adaptation to the climate change, Renew. Energy. 101 (2017) 1226–1241. doi:https://doi.org/10.1016/j.renene.2016.09.064.
[51] K.K.W. Wan, D.H.W. Li, J.C. Lam, Assessment of climate change impact on building energy use and mitigation measures in subtropical climates, Energy. 36 (2011) 1404–1414. doi:https://doi.org/10.1016/j.energy.2011.01.033.
[52] A. Roetzel, A. Tsangrassoulis, Impact of climate change on comfort and energy performance in offices, Build. Environ. 57 (2012) 349–361. doi:https://doi.org/10.1016/j.buildenv.2012.06.002.
[53] A. Roetzel, A. Tsangrassoulis, U. Dietrich, Impact of building design and occupancy on office comfort and energy performance in different climates, Build. Environ. 71 (2014) 165–175. doi:https://doi.org/10.1016/j.buildenv.2013.10.001.
[54] D. Sánchez-García, C. Rubio-Bellido, M. Marrero Meléndez, F.J. Guevara-García, J. Canivell, El control adaptativo en instalaciones existentes y potencial en el contexto del cambio climatico, Hábitat Sustentable. 7 (2017) 6–17. doi:10.22320/07190700.2017.07.02.01.

[55] K.K.W. Wan, D.H.W. Li, W. Pan, J.C. Lam, Impact of climate change on building energy use in different climate zones and mitigation and adaptation implications, Appl. Energy. 97 (2012) 274–282. doi:https://doi.org/10.1016/j.apenergy.2011.11.048.

[56] A. Jiang, A. O'Meara, Accommodating thermal features of commercial building systems to mitigate energy consumption in Florida due to global climate change, Energy Build. 179 (2018) 86–98. doi:https://doi.org/10.1016/j.enbuild.2018.08.046.

[57] L. Guan, Energy use, indoor temperature and possible adaptation strategies for air-conditioned office buildings in face of global warming, Build. Environ. 55 (2012) 8–19. doi:https://doi.org/10.1016/j.buildenv.2011.11.013.

[58] T. Berger, C. Amann, H. Formayer, A. Korjenic, B. Pospischal, C. Neururer, R. Smutny, Impacts of climate change upon cooling and heating energy demand of office buildings in Vienna, Austria, Energy Build. 80 (2014) 517–530. doi:https://doi.org/10.1016/j.enbuild.2014.03.084.

[59] T. Berger, C. Amann, H. Formayer, A. Korjenic, B. Pospichal, C. Neururer, R. Smutny, Impacts of urban location and climate change upon energy demand of office buildings in Vienna, Austria, Build. Environ. 81 (2014) 258–269. doi:https://doi.org/10.1016/j.buildenv.2014.07.007.

[60] A. Walsh, D. Cóstola, L.C. Labaki, Performance-based validation of climatic zoning for building energy efficiency applications, Appl. Energy. 212 (2018) 416–427. doi:https://doi.org/10.1016/j.apenergy.2017.12.044.

[61] F. Martín-Consuegra, A.H. Aja, I.O.S. José, C. Alonso, Energy needs and vulnerability estimation at an urban scale for residential neighbourhoods heating in Madrid (Spain), Proc. PLEA 2016 Los Angeles - 32th Int. Conf. Passiv. Low Energy Archit. Cities, Build. People Towar. Regen. Environ. 3 (2016) 1413–1418.

[62] S.C. Taylor, S.K. Firth, C. Wang, D. Allinson, M. Quddus, P. Smith, Spatial mapping of building energy demand in Great Britain, GCB Bioenergy. 6 (2014) 123–135. doi:10.1111/gcbb.12165.

[63] C. Rubio-Bellido, A. Pérez-Fargallo, J.A. Pulido-Arcas, Optimization of annual energy demand in office buildings under the influence of climate change in Chile, Energy. 114 (2016) 569–585. doi:https://doi.org/10.1016/j.energy.2016.08.021.

[64] C. Rubio-Bellido, A. Pérez-Fargallo, J.A. Pulido-Arcas, M. Trebilcock, Application of adaptive comfort behaviors in Chilean social housing standards under the influence of climate change, Build. Simul. 10 (2017) 933–947. doi:10.1007/s12273-017-0385-9.

[65] K. Verichev, M. Carpio, Climatic zoning for building construction in a temperate climate of Chile, Sustain. Cities Soc. 40 (2018) 352–364. doi:10.1016/j.scs.2018.04.020.

[66] A. Yezioro, B. Dong, F. Leite, An applied artificial intelligence approach towards assessing building performance simulation tools, Energy Build. 40 (2008) 612–620. doi:10.1016/j.enbuild.2007.04.014.

[67] F.H. Abanda, L. Byers, An investigation of the impact of building orientation on energy consumption in a domestic building using emerging BIM (Building Information Modelling), Energy. 97 (2016) 517–527. doi:10.1016/j.energy.2015.12.135.

[68] K. Aljundi, A. Pinto, F. Rodrigues, Energy Analysis Using Cooperation Between Bim Tools (Revit and Green Building Studio) and Energy Plus, 1º Congr. Port. Build. Inf.

Model. (2016) 309–319. doi:10.5281/zenodo.166758.
[69] S. Kim, J.-H. Woo, Analysis of the differences in energy simulation results between Building Information Modeling (BIM)-based simulation method and the detailed simulation method, in: Proc. 2011 Winter Simul. Conf., 2011: pp. 3550–3561.
[70] T. Reeves, S. Olbina, R. Issa, VALIDATION OF BUILDING ENERGY MODELING TOOLS: ECOTECT™, GREEN BUILDING STUDIO™ AND IES<VE>™, in: Proc. 2012 Winter Simul. Conf., 2012: pp. 1219–1229.
[71] N. Mostafavi, M. Farzinmoghadam, S. Hoque, Envelope retrofit analysis using eQUEST, IESVE Revit Plug-in and Green Building Studio: a university dormitory case study, Int. J. Sustain. Energy. 34 (2015) 594–613. doi:10.1080/14786451.2013.848207.
[72] T. Reeves, S. Olbina, R.R.A. Issa, Guidelines for using building information modeling for energy analysis of buildings, Buildings. 5 (2015) 1361–1388. doi:10.3390/buildings5041361.
[73] M. Jamnický, Green Building Studio Test Result Comparison with Test from ANSI ASHARE Standard 140-2011, Adv. Mater. Res. 1057 (2014) 11–18. doi:10.4028/www.scientific.net/AMR.1057.11.
[74] E. Kamel, A.M. Memari, Review of BIM's application in energy simulation: Tools, issues, and solutions, Autom. Constr. 97 (2019) 164–180. doi:https://doi.org/10.1016/j.autcon.2018.11.008.
[75] P. Singh, A. Sadhu, Multicomponent energy assessment of buildings using building information modeling, Sustain. Cities Soc. 49 (2019) 101603. doi:https://doi.org/10.1016/j.scs.2019.101603.
[76] A. Alwisy, B. Barkokebas, S.B. Hamdan, M. Gül, M. Al-Hussein, Energy-based target cost modelling for construction projects, J. Build. Eng. 20 (2018) 387–399. doi:https://doi.org/10.1016/j.jobe.2018.06.010.
[77] M. Najjar, K. Figueiredo, M. Palumbo, A. Haddad, Integration of BIM and LCA: Evaluating the environmental impacts of building materials at an early stage of designing a typical office building, J. Build. Eng. 14 (2017) 115–126. doi:https://doi.org/10.1016/j.jobe.2017.10.005.
[78] S.O. Ajayi, L.O. Oyedele, O.M. Ilori, Changing significance of embodied energy: A comparative study of material specifications and building energy sources, J. Build. Eng. 23 (2019) 324–333. doi:https://doi.org/10.1016/j.jobe.2019.02.008.
[79] H. Kim, A. Stumpf, W. Kim, Analysis of an energy efficient building design through data mining approach, Autom. Constr. 20 (2011) 37–43. doi:https://doi.org/10.1016/j.autcon.2010.07.006.
[80] S.O. Ajayi, L.O. Oyedele, B. Ceranic, M. Gallanagh, K.O. Kadiri, Life cycle environmental performance of material specification: a BIM-enhanced comparative assessment, Int. J. Sustain. Build. Technol. Urban Dev. 6 (2015) 14–24. doi:10.1080/2093761X.2015.1006708.
[81] K.S. Abhinaya, V.R. Prasath Kumar, L. Krishnaraj, Assessment and remodelling of a conventional building into a green building using BIM, Int. J. Renew. Energy Res. 7 (2017) 1675–1681.
[82] N. Thakur, V.R. Prasath Kumar, M. Balasubramanian, Comparative energy audit of building models using BIM for the sustainable development, J. Adv. Res. Dyn. Control Syst. 10 (2018) 986–992.
[83] Y. Bahar, C. Pere, J. Landrieu, C. Nicolle, A Thermal Simulation Tool for Building

and Its Interoperability through the Building Information Modeling (BIM) Platform, Buildings. 3 (2013) 380–398. doi:10.3390/buildings3020380.
[84] G. Grell, J. Dudhia, D.R. Stauffer, A description of the Fifth-generation Penn State/NCAR Mesoscale Model (MM5), 1994. doi:10.5065/D60Z716B.
[85] ESRI, ArcGIS, (2019). http://desktop.arcgis.com/es/arcmap/ (accessed October 6, 2019).
[86] INE, Instituto Nacional de Estadística de Chile, 2018.
[87] Chile, Biblioteca del Congreso Nacional de Chile, Información Territorial, (2019). https://www.bcn.cl/siit/nuestropais/regiones (accessed April 6, 2019).
[88] Chile, Dirección Meteorológica de Chile - Dirección General de Aeronáutica Civil, (2019). http://www.meteochile.gob.cl/PortalDMC-web/index.xhtml (accessed April 6, 2019).
[89] Chile, Ministry of Housing and Urban Planning of Chile - Manual de Aplicación, Reglamentación Térmica, Ordenanza General de Urbanismo y Construcciones (art. 4.1.10), par. I-IV, Ministerio de Vivienda y Urbanismo de Chile, 2006.
[90] Chile, Ministry of Housing and Urban Planning of Chile - Ordenanza General de Urbanismo y Construcciones, Ministerio de Vivienda y Urbanismo de Chile. Decreto Supremo №47 de 1992. D.O. de 13.04.09, 2009.
[91] American Society of Heating Refrigerating and Air-Conditioning Engineers Inc. [ASHRAE], ANSI/ASHRAE 169-2013 Climatic Data For Building Design Standards, 2013.
[92] Chile, Center of Climate and Resilience Research CR(2) Explorador Climático, (2019). http://explorador.cr2.cl/ (accessed October 18, 2019).
[93] K. Verichev, M. Zamorano, M. Carpio, Assessing the applicability of various climatic zoning methods for building construction: Case study from the extreme southern part of Chile, Build. Environ. 160 (2019) 106165. doi:10.1016/J.BUILDENV.2019.106165.
[94] Chile, Center of Climate and Resilience Research CR(2) Centro Fondap Conicyt sobre clima, cambio climático y resiliencia, (2019). http://www.cr2.cl/ (accessed October 6, 2019).
[95] WCRP, World Climate Research Programme - Coupled Model Intercomparison Project (CMIP) - Overview, (2019). https://www.wcrp-climate.org/wgcm-cmip (accessed October 6, 2019).
[96] A. Jiang, Y. Zhu, A. Elsafty, M. Tumeo, Effects of Global Climate Change on Building Energy Consumption and Its Implications in Florida, Int. J. Constr. Educ. Res. 14 (2018) 22–45. doi:10.1080/15578771.2017.1280104.
[97] S.E. Belcher, J.N. Hacker, D.S. Powell, Constructing design weather data for future climates, Build. Serv. Eng. Res. Technol. 26 (2005) 49–61. doi:10.1191/0143624405bt112oa.
[98] M.A. Oliver, R. Webster, Kriging: a method of interpolation for geographical information systems, Int. J. Geogr. Inf. Syst. 4 (1990) 313–332. doi:10.1080/02693799008941549.
[99] L.M. López-Ochoa, K. Verichev, J. Las-Heras-Casas, M. Carpio, Solar domestic hot water regulation in the Latin American residential sector with the implementation of the Energy Performance of Buildings Directive: The case of Chile, Energy. 188 (2019) 115985. doi:https://doi.org/10.1016/j.energy.2019.115985.
[100] C. Molina, M. Kent, I. Hall, B. Jones, A data analysis of the Chilean housing stock

and the development of modelling archetypes, Energy Build. 206 (2020) 109568. doi:https://doi.org/10.1016/j.enbuild.2019.109568.
[101] B. Purushothama, 9 - Maintenance of humidity, in: B.B.T.-H. and V.M. in T.I. Purushothama (Ed.), Woodhead Publishing India, 2009: pp. 121–161. doi:https://doi.org/10.1533/9780857092847.121.
[102] S.M. Levy, Section 12 - Electrical Formulas and Calculations, in: S.M.B.T.-C.C.M. Levy (Ed.), Butterworth-Heinemann, Boston, 2012: pp. 635–671. doi:https://doi.org/10.1016/B978-0-12-382243-7.00014-0.
[103] Autodesk, Autodesk knowledgw network; Revit products; HVAC systems, (2019). https://knowledge.autodesk.com/support/revit-products/learn-explore/caas/CloudHelp/cloudhelp/2015/ENU/Revit-Analyze/files/GUID-38A9EB5B-8631-43B4-9AD6-6F532BC860D8-htm.html (accessed November 26, 2019).
[104] Ministerio de Vivienda y Urbanismo -MINVU, Estándares de construccíon sustentable para viviendas de Chile. Tomo I. Salud y bienestar., Santiago, 2018.
[105] Y. Olaya, F. Vásquez, D.B. Müller, Dwelling stock dynamics for addressing housing deficit, Resour. Conserv. Recycl. 123 (2017) 187–199. doi:https://doi.org/10.1016/j.resconrec.2016.09.028.
[106] M. Martin, N.H. Wong, D.J.C. Hii, M. Ignatius, Comparison between simplified and detailed EnergyPlus models coupled with an urban canopy model, Energy Build. 157 (2017) 116–125. doi:https://doi.org/10.1016/j.enbuild.2017.01.078.
[107] A. Moreno, A. Riverola, D. Chemisana, Energetic simulation of a dielectric photovoltaic-thermal concentrator, Sol. Energy. 169 (2018) 374–385. doi:https://doi.org/10.1016/j.solener.2018.04.037.
[108] D.A. Vasco, M. Muñoz-Mejías, R. Pino-Sepúlveda, R. Ortega-Aguilera, C. García-Herrera, Thermal simulation of a social dwelling in Chile: Effect of the thermal zone and the temperature-dependant thermophysical properties of light envelope materials, Appl. Therm. Eng. 112 (2017) 771–783. doi:10.1016/j.applthermaleng.2016.10.130.
[109] K. Verichev, A. Salimova, M. Carpio, Thermal and climatic zoning for construction in the southern part of Chile, Adv. Sci. Res. 15 (2018) 63–69. doi:10.5194/asr-15-63-2018.
[110] D. Conradie, T. van Reenen, S. Bole, Degree-day building energy reference map for South Africa, Build. Res. Inf. 46 (2018) 191–206. doi:10.1080/09613218.2016.1252619.

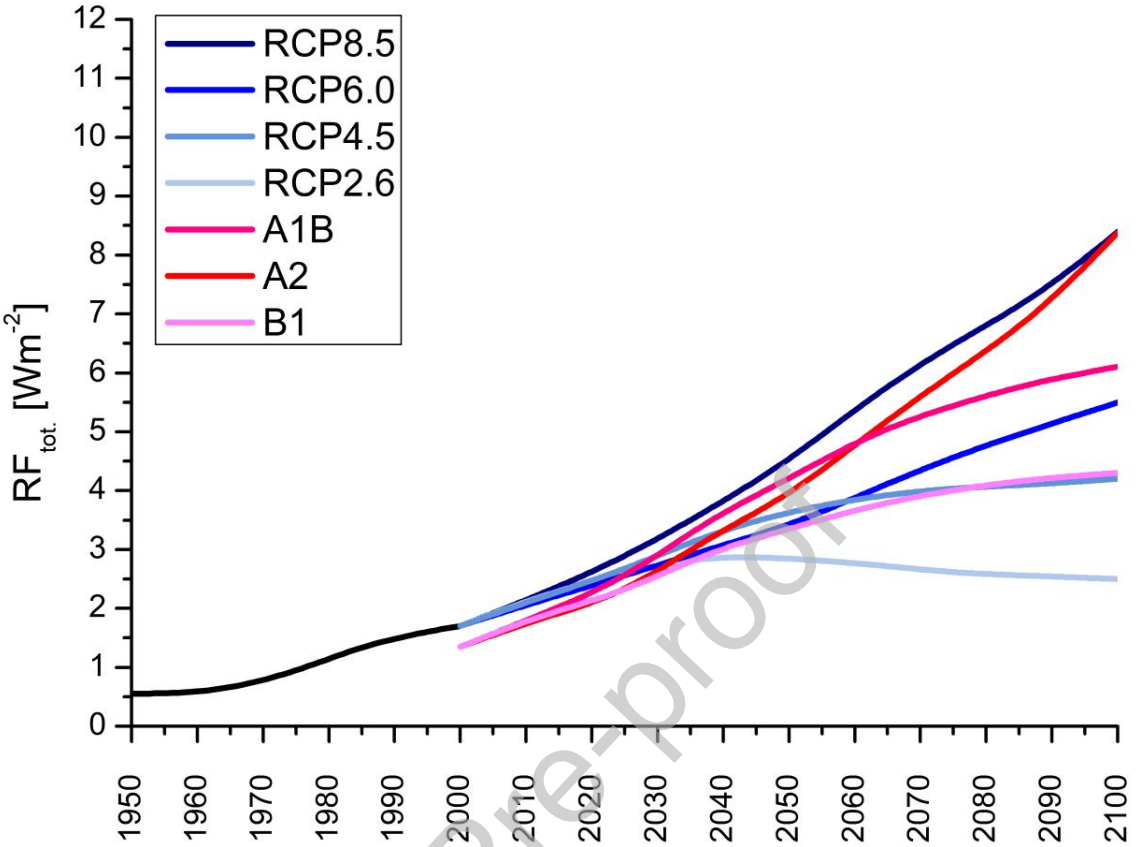

Fig. 1. Compliance between RCP and SRES scenarios based on total RF of the global climatic system.

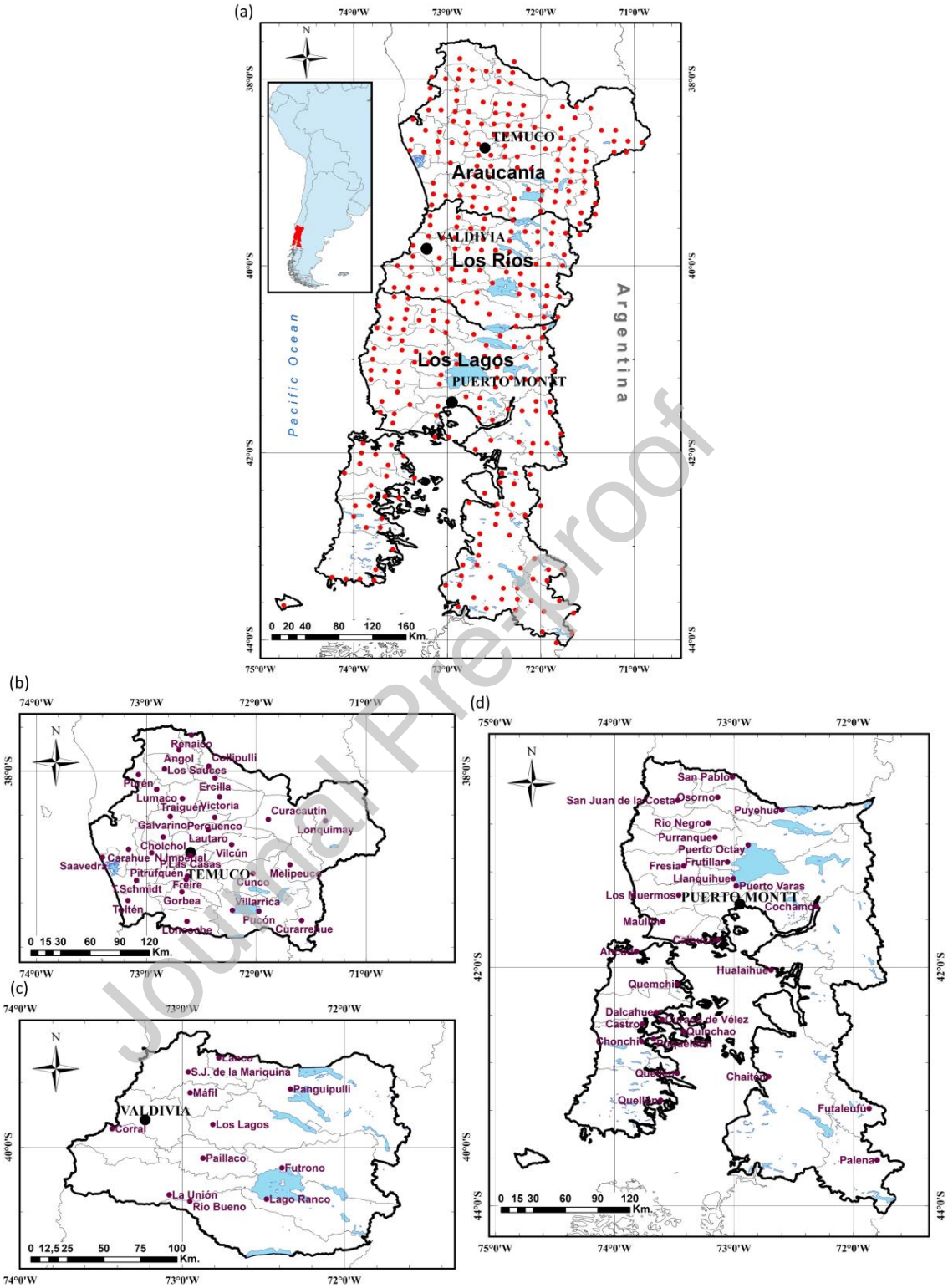

Fig. 2. Map of general location of study area with geographical locations for energy simulation (red dots) (a) and location of principal cities of communes (b-d).

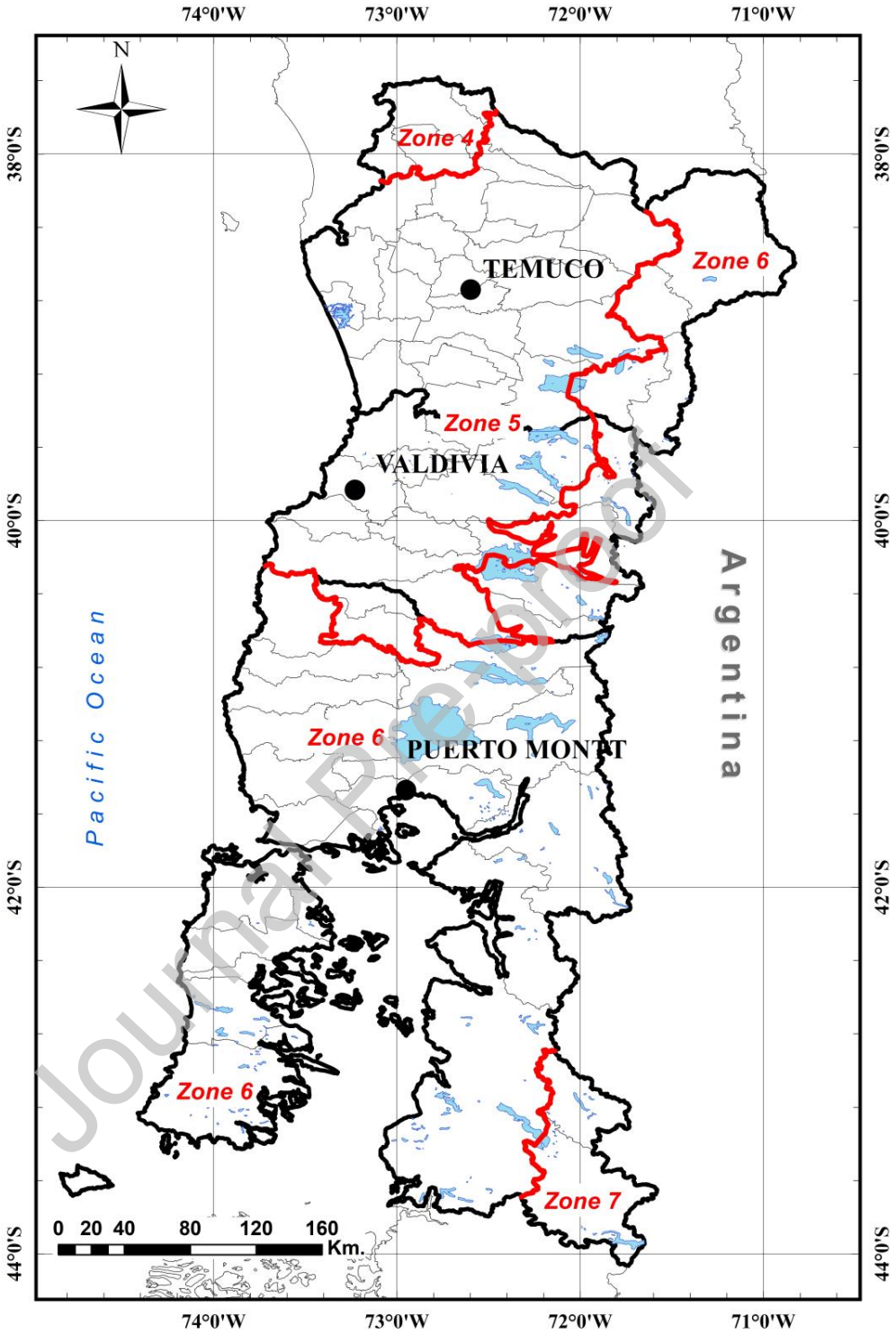

Fig. 3. Thermal zones by the RT OGUC document (1999). Zone definition depends on annual value of HDD15°C (Table 2).

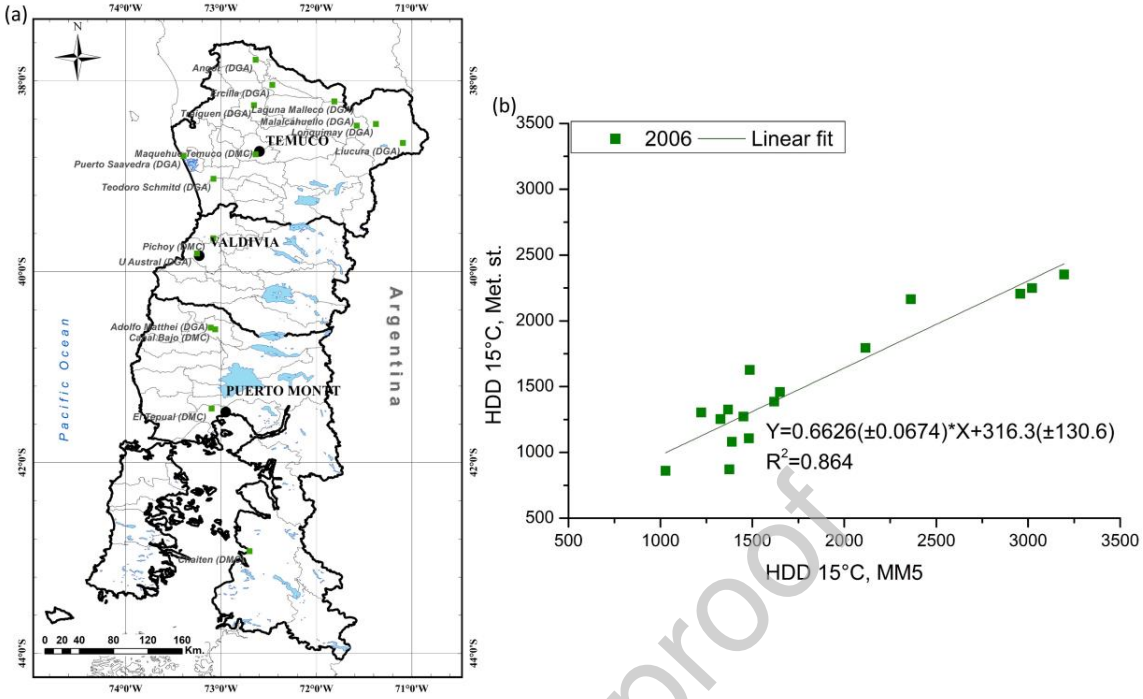

Fig. 4. Map of geographical location of meteorological stations (a) and correlation of annual values of HDD15°C from the meteorological stations and HDD15°C from the MM5 (slope and intercept of the regression line with standard errors) (b).

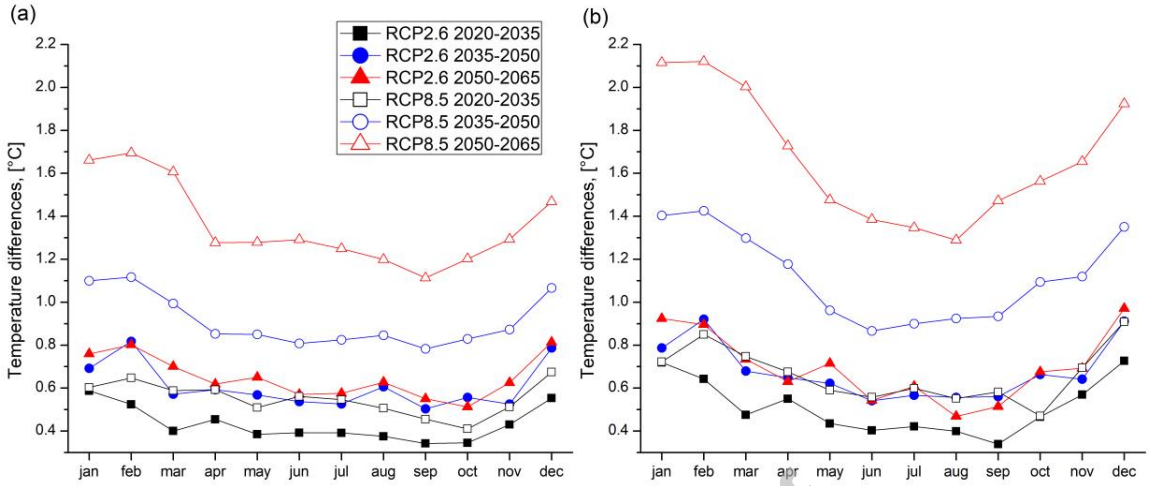

Fig. 5. Monthly values of differences in monthly average minimum (a) and maximum(b) temperatures between future periods and baseline climate.

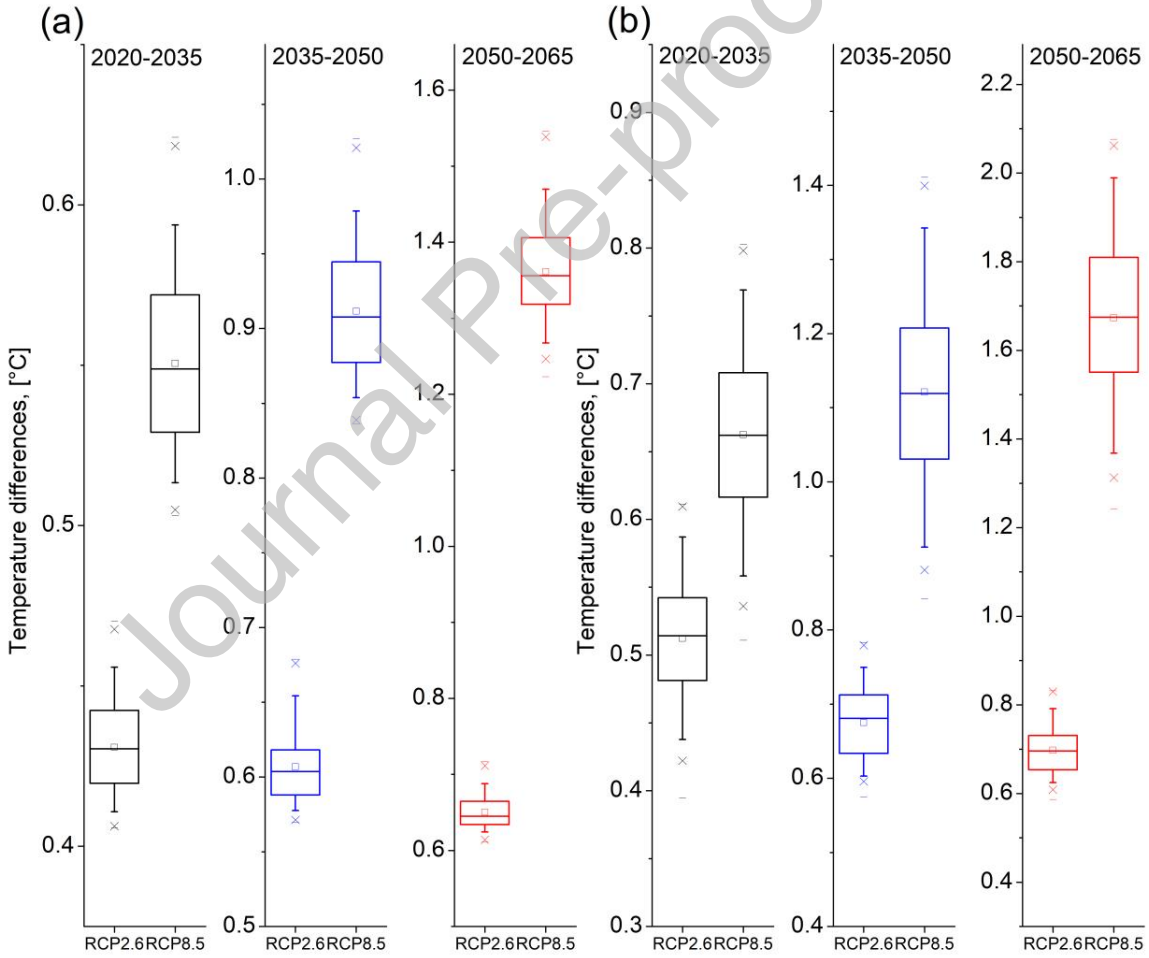

Fig. 6. Box-plots of variability of the values of expected changes in annual average minimum (a) and maximum (b) temperatures compared to the baseline climate for the study area. Box range – 25-75%, whisker range – 5-95%, asterisk range – 1-99% and min-max.

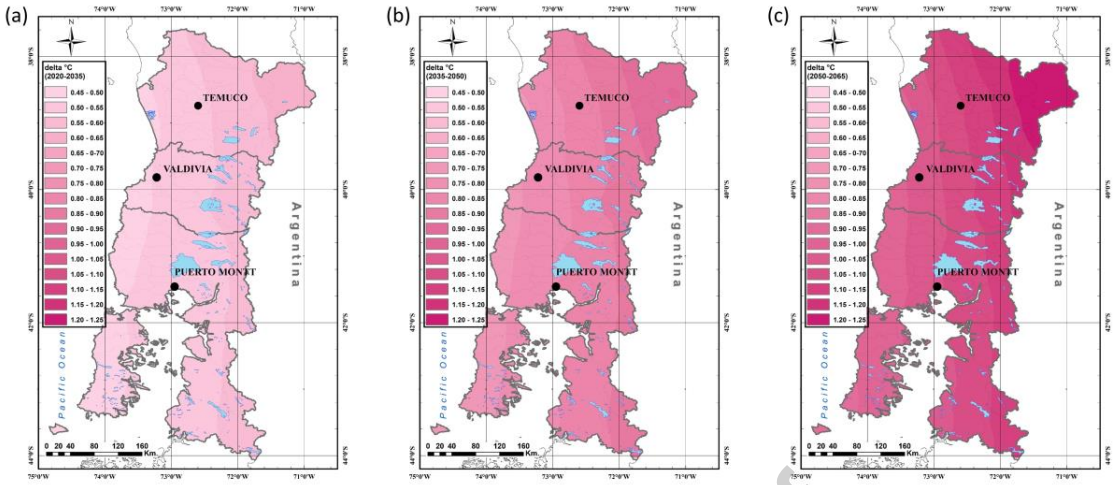

Fig. 7. Change in the annual average temperature in future periods (a) 2020–2035, (b) 2035–2050 and (c) 2050–2065, as compared to baseline climate (average of the RCP2.6 and RCP8.5 scenarios).

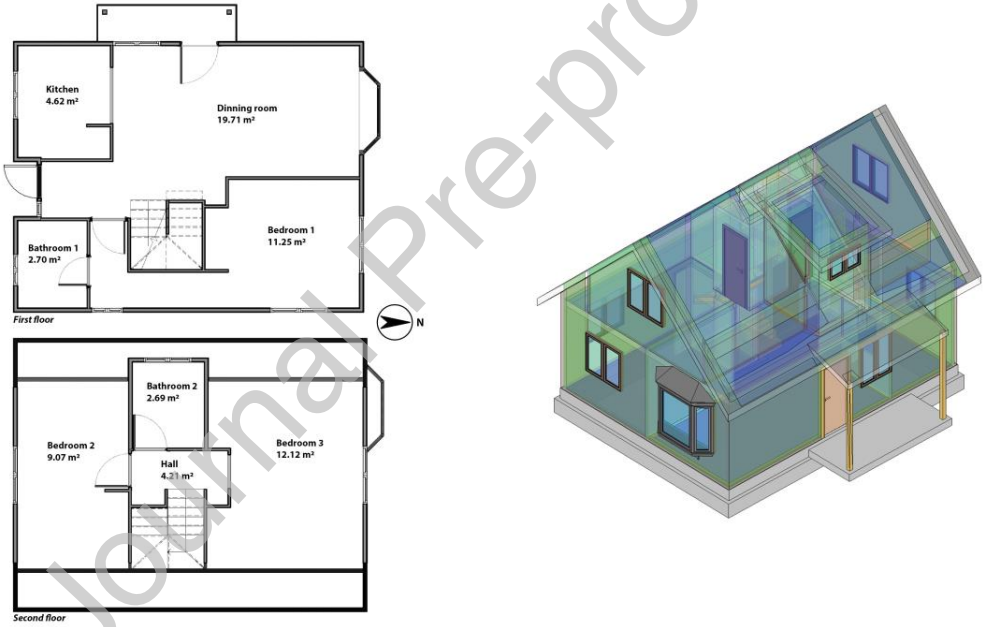

Fig. 8. Type of simulated dwelling.

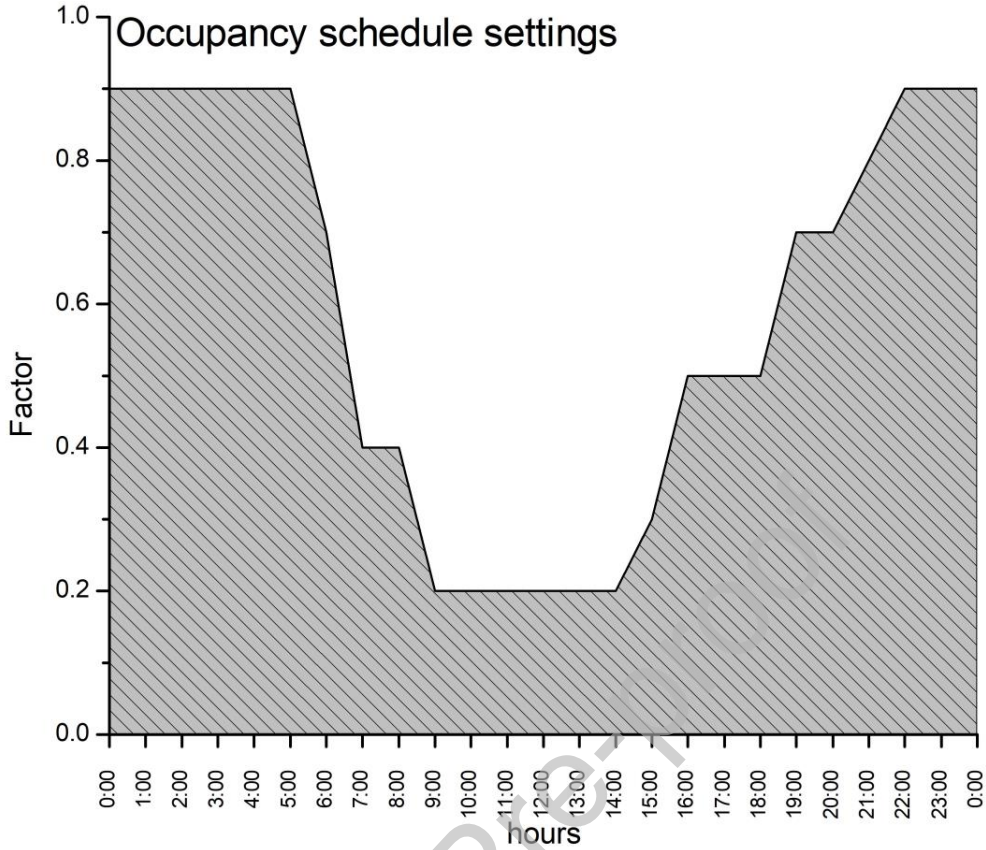

Fig. 9. Dwelling occupancy schedule settings for energy simulation.

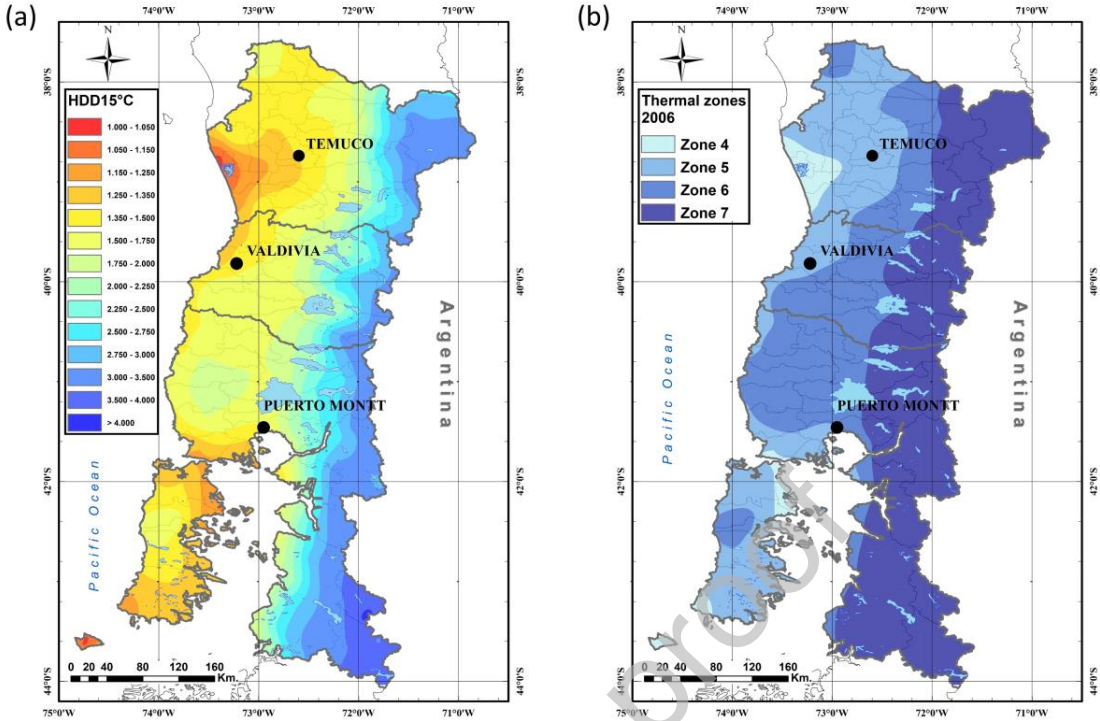

Fig. 10. Map of HDD15°C (a) and thermal zones of the RT OGUC (b) by MM5 data in baseline climate period (2006).

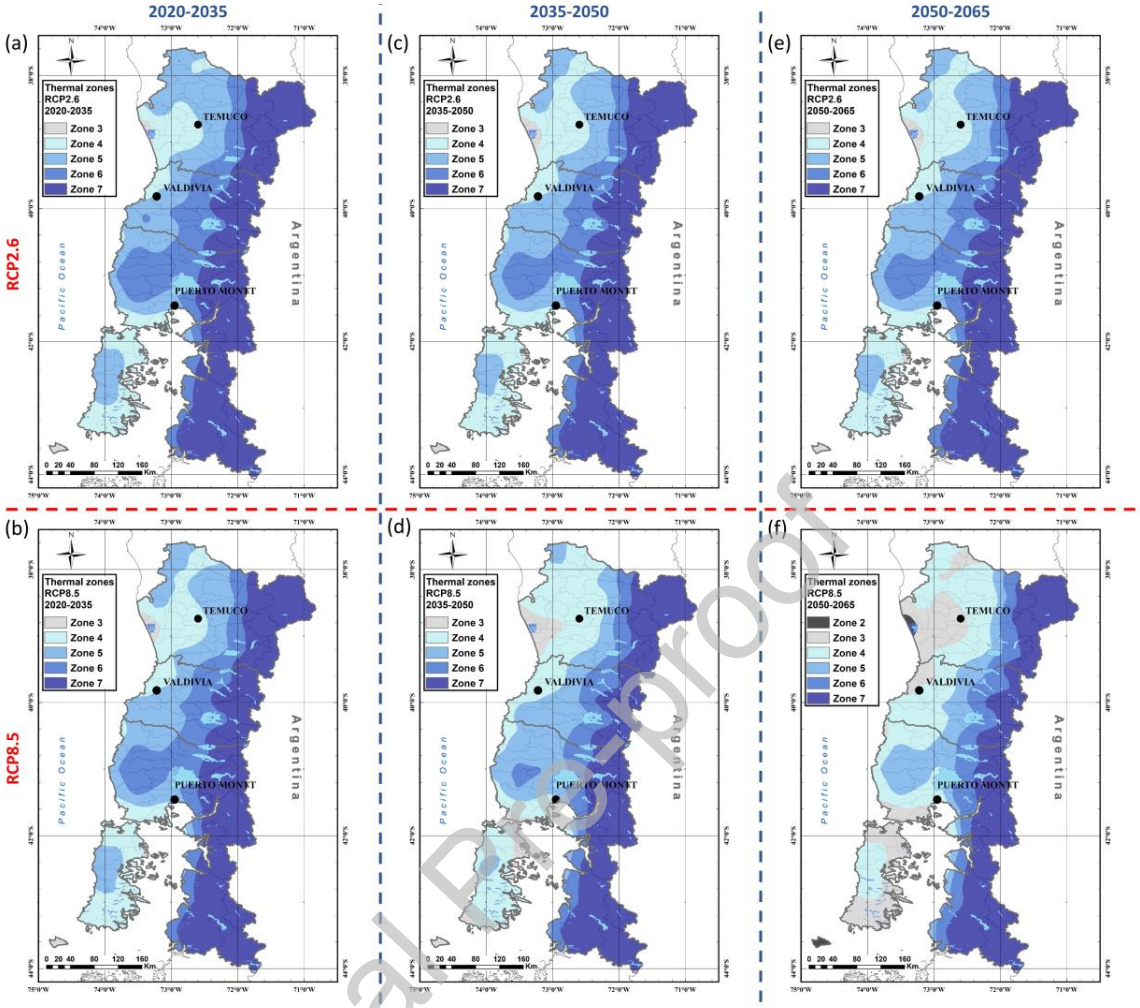

Fig. 11. RT OGUC thermal zones in future periods (a, b) 2020–2035; (c, d) 2035–2050; (e, f) 2050–2065) for scenarios RCP2.6 and RCP8.5, respectively.

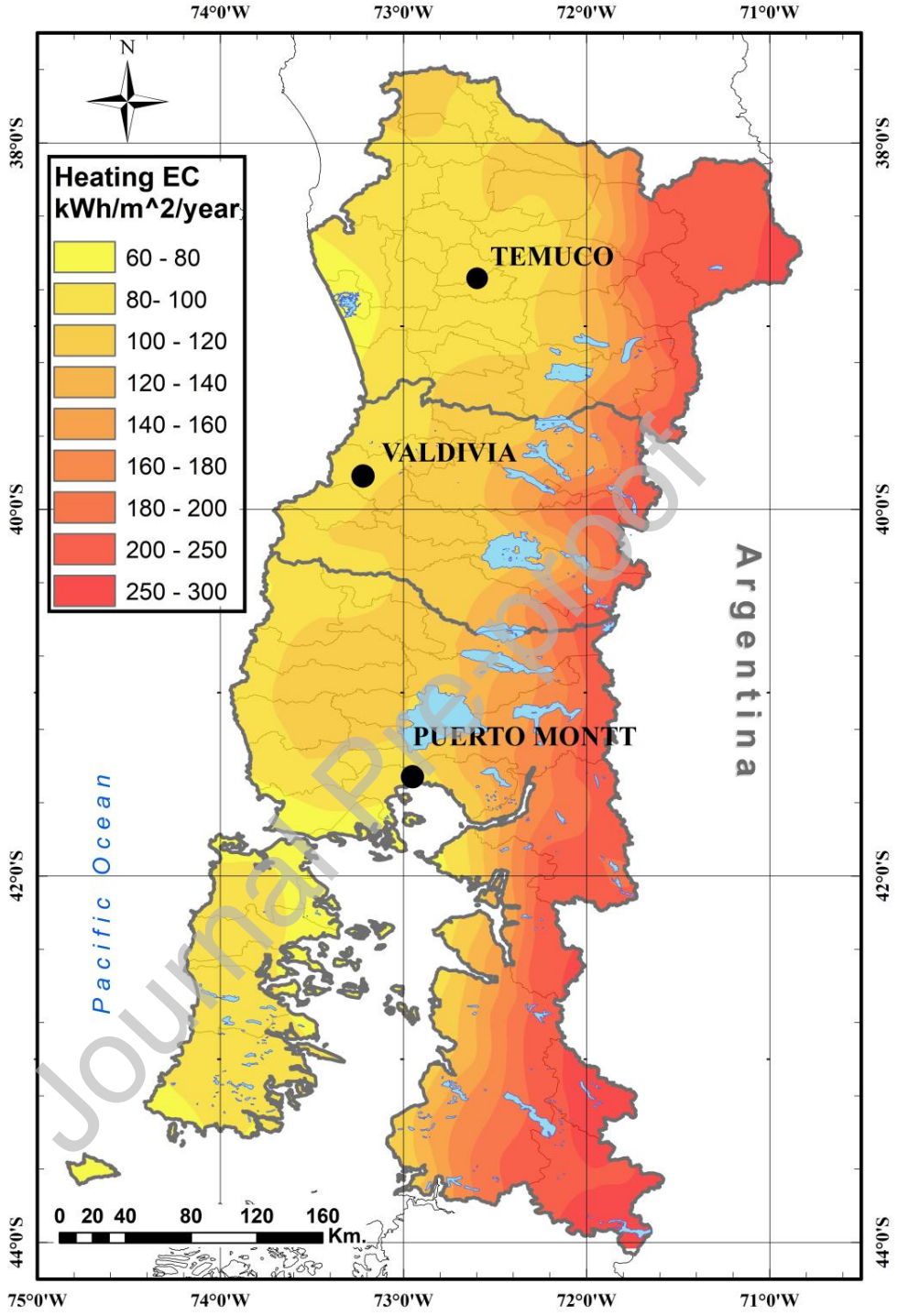

Fig. 12. Results of heating EC simulation in the baseline climate period.

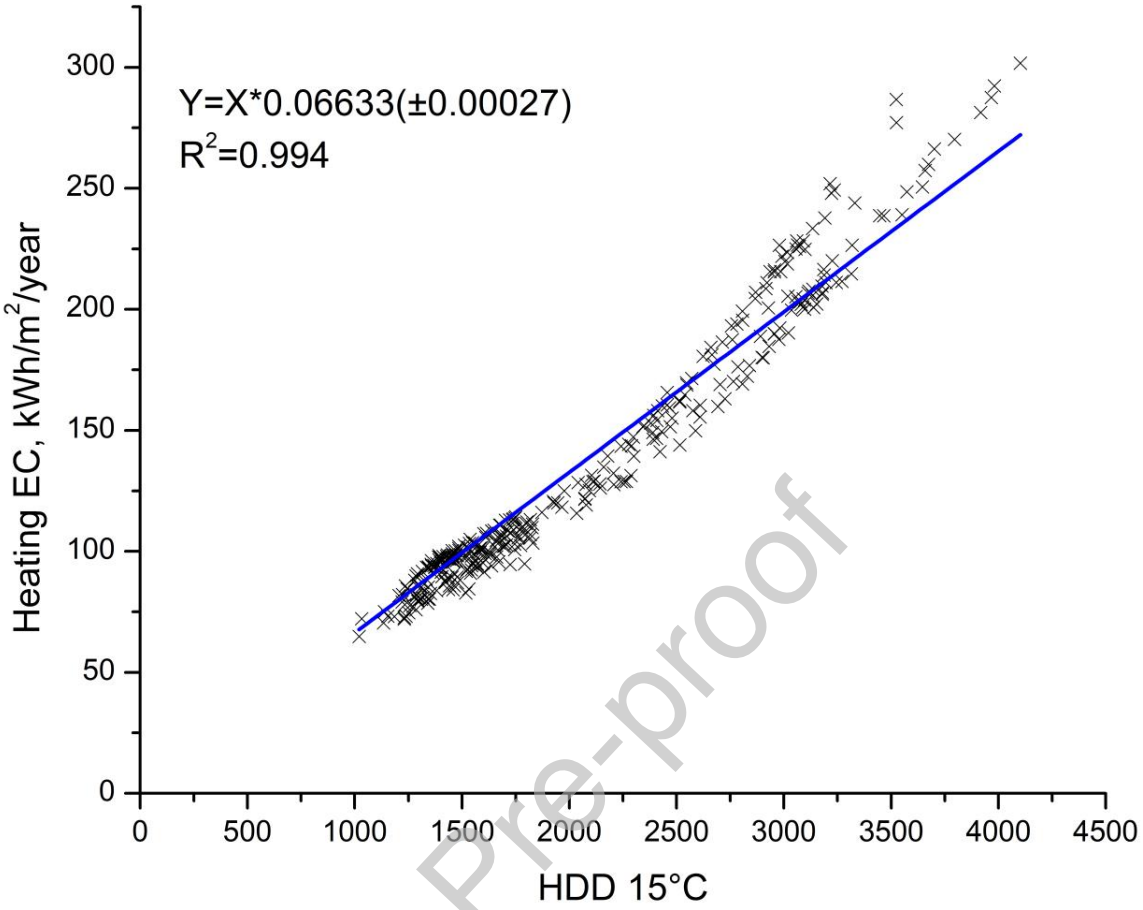

Fig. 13. Correlation between heating EC and annual value of HDD15°C in 360 geographical locations in baseline climate period (slope of the regression line with standard error).

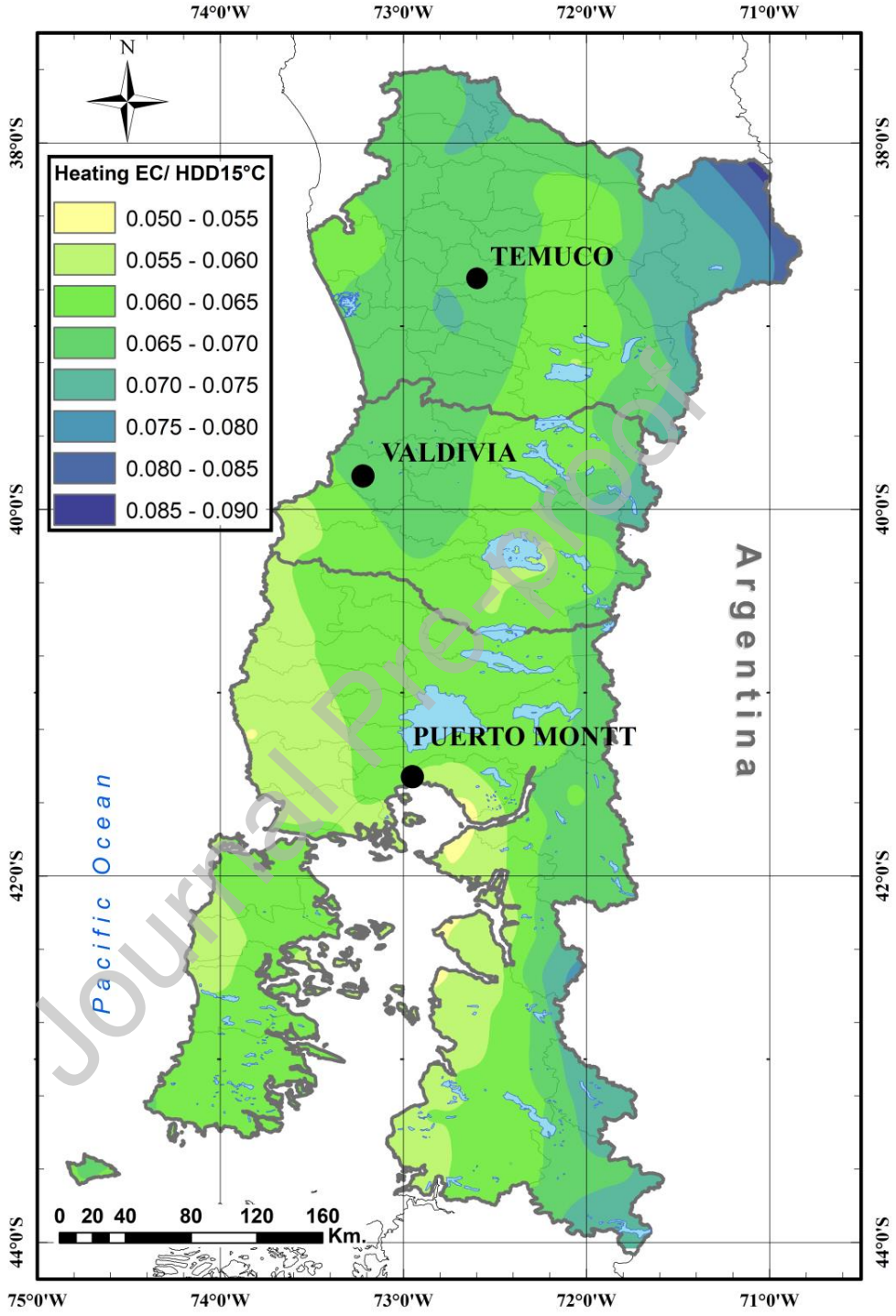

Fig. 14. Spatial distribution of the quotient between heating EC and HDD15°C [kWh/m^2/year/HDD15°C] in the baseline climate period.

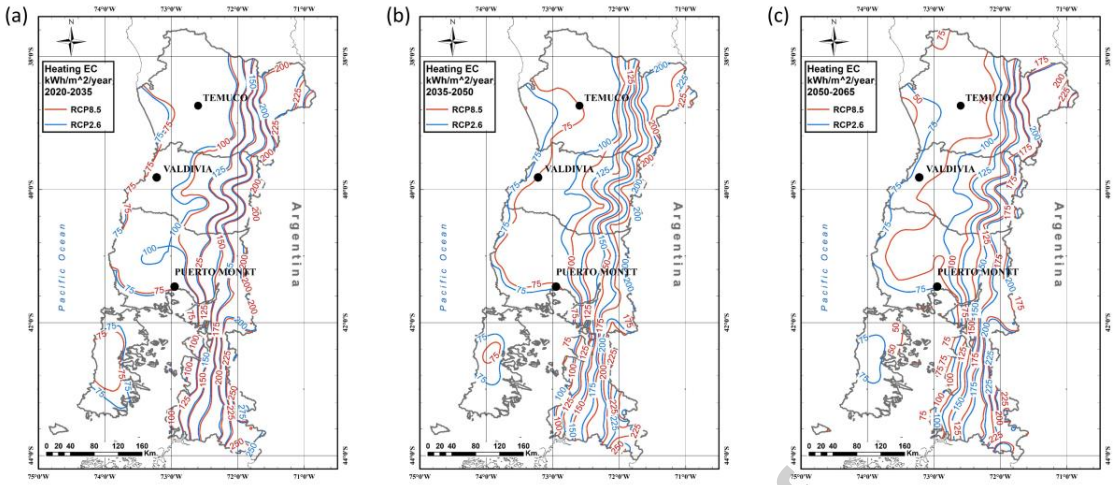

Fig. 15. Estimated heating EC in the dwelling under study in future periods (a) 2020–2035, (b) 2035–2050 and (c) 2050–2065).

Table 1. Revised publications with SRES and RCP scenarios.

Scenario		References
SRES scenarios		
A1	A1FI	[35,38]
	A1T	—
	A1B	[30,31,34,35,51]
A2		[30,32,52–54,33,36–42]
B1		[30,31,38,41,51,55]
B2		[39]
RCP scenarios		
RCP2.6		[45,47]
RCP4.5		[43,44,47,48,50]
RCP6.0		[45,47]
RCP8.5		[43–47,49]

Table 2. Thermals zones of Chile, thermal transmittance (U-value) and maximum percentage area of glazed surfaces according to RT OGUC for each thermal zone.

Thermal zone		**1**	**2**	**3**	**4**	**5**	**6**	**7**
Value of annual HDD15℃		≤ 500	>500 ≤750	>750 ≤1000	>1000 ≤1250	>1250 ≤1500	>1500 ≤2000	> 2000
Walls	U [W/m²·K]	4.0	3.0	1.9	1.7	1.6	1.1	0.6
Roof	U [W/m²·K]	0.84	0.60	0.47	0.38	0.33	0.28	0.25
Floor	U [W/m²·K]	3.60	0.86	0.70	0.60	0.50	0.39	0.32
Monolithic glass [%]		50	40	25	21	18	14	12
Hermetic double glazed windows [%]	3.6 ⩾ U [W/m²·K] > 2.4	60	60	60	60	51	37	28
	U [W/m²·K] > 2.4	80	80	80	75	70	55	37

Table 3. Annual average HDD15°C values from meteorological stations and MM5 (2006).

Lat.	Lon.	Name of Met. st.	Alt. (m)	HDD15°C	
				Met. st.	MM5
-37.7794	-72.6372	Angol (DGA)	113	872	1375
-38.0442	-72.4611	Ercilla (DGA)	262	1107	1482
-38.2156	-71.8106	Laguna Malleco (DGA)	894	2165	2362
-38.6517	-71.0919	Liucura (DGA)	1043	2351	3196
-38.4536	-71.3742	Lonquimay (DGA)	931	2248	3022
-38.4703	-71.5753	Malalcahuello (DGA)	950	2205	2958
-38.7700	-72.6369	Maquehue Temuco (DMC)	92	1253	1327
-38.7886	-73.3936	Puerto Saavedra (DGA)	5	861	1028
-39.0278	-73.0781	Teodoro Schmitd (DGA)	13	1303	1223
-38.2561	-72.6536	Traiguen (DGA)	234	1272	1452
-39.6506	-73.0808	Pichoy (DMC)	21	1325	1368
-39.8103	-73.2517	U. Austral (DGA)	10	1081	1389
-40.5883	-73.1069	Adolfo Matthei (DGA)	55	1386	1619
-40.6050	-73.0608	Canal Bajo (DMC)	61	1459	1650
-42.9303	-72.7008	Chaiten (DMC)	10	1794	2116
-41.4350	-73.0978	El Tepual (DMC)	16	1628	1486

Table 4. List of climatic models used in the research.

Model	Modelling group (or centre)	Type	RCP2.6	RCP8.5
ACCESS1-0	Commonwealth Scientific and Industrial Research Organisation/Bureau of Meteorology, Australia	global		+
ACCESS1-3	Commonwealth Scientific and Industrial Research Organisation/Bureau of Meteorology, Australia	global		+
bcc-csm1-1	Beijing Climate Center Climate System Model	global	+	+
bcc-csm1-1-m	Beijing Climate Center Climate System Model	global	+	+
BNU-ESM	Beijing Normal University, China	global	+	+
CanESM2	Canadian Centre for Climate Modelling and Analysis, Canada	global	+	+
CCSM4	National Center for Atmospheric Research, USA	global	+	+
CESM1-BGC	National Science Foundation, Department of Energy, National Center for Atmospheric Research, USA	global		+
CESM1-CAM5	National Science Foundation, Department of Energy, National Center for Atmospheric Research, USA	global	+	+
CESM1-CAM5-1-FV2	National Science Foundation, Department of Energy, National Center for Atmospheric Research, USA	global		+
CMCC-CESM	Centro Euro-Mediterraneo per I Cambiamenti Climatici, Italy	global		+
CMCC-CM	Centro Euro-Mediterraneo per I Cambiamenti Climatici, Italy	global		+
CMCC-CMS	Centro Euro-Mediterraneo per I Cambiamenti Climatici, Italy	global		+
CNRM-CM5	Centre National de Recherches Météorologiques, Centre Européen de Recherche et de Formation Avancée en Calcul Scientifique, France	global	+	+
CSIRO-Mk3-6-0	Commonwealth Scientific and Industrial Research Organisation/Queensland Climate Change Centre of Excellence, Australia	global	+	+
DMC-WRF@MIROC5	Forecasts WRF from Chile DMC: Dirección Meteorológica de Chile	local	+	+
FGOALS-g2	State Key Laboratory Numerical Modeling for atmospheric Science and geophysical Fluid Dynamics, China	global	+	+
FIO-ESM	The First Institute of Oceanography, SOA, China	global	+	+
GISS-E2-H	NASA/GISS (Goddard Institute for Space Studies), USA	global	+	+
GISS-E2-H-CC	NASA/GISS (Goddard Institute for Space Studies), USA	global		+
GISS-E2-R	NASA/GISS (Goddard Institute for Space Studies), USA	global	+	+
GISS-E2-R-CC	NASA/GISS (Goddard Institute for Space Studies), USA	global		+
HadGEM2-AO	Met Office Hadley Centre, UK	global	+	+
HadGEM2-CC	Met Office Hadley Centre, UK	global		+
HadGEM2-ES	Met Office Hadley Centre, UK	global	+	+
inmcm4	Russian Academy of Sciences, Institute of Numerical Mathematics, Russian Federation	global		+
IPSL-CM5A-MR	Institut Pierre Simon Laplace, France	global	+	+
IPSL-CM5B-LR	Institut Pierre Simon Laplace, France	global		+
MIROC4h	Atmosphere and Ocean Research Institute, National Institute for Environmental Studies and Japan Agency for Marine-Earth Science and Technology, Japan	global		+
MIROC5	Atmosphere and Ocean Research Institute, National Institute for Environmental Studies and Japan Agency for Marine-Earth Science and Technology, Japan	global	+	+
MIROC-ESM	Atmosphere and Ocean Research Institute, National Institute for Environmental Studies and Japan Agency for Marine-Earth Science and Technology, Japan	global	+	+
MIROC-ESM-CHEM	Atmosphere and Ocean Research Institute, National Institute for Environmental Studies and Japan Agency for Marine-Earth Science and Technology, Japan	global	+	+
MPI-ESM-LR	Max Planck Institute for Meteorology, Germany	global	+	+
MPI-ESM-MR	Max Planck Institute for Meteorology, Germany	global	+	+
MRI-CGCM3	Meteorological Research Institute, Japan	global	+	+
MRI-ESM1	Meteorological Research Institute, Japan	global		+
NorESM1-M	Bjerknes Centre for Climate Research, Norwegian Meteorological Institute, Norway	global	+	+
RegCM4@MPI-M-MPI-ESM-MR	National Center for Atmospheric Research, USA	local	+	+
SMHI-RCA4@CCCma-CanESM2	Swedish Meteorological and Hydrological Institute	regional		+
SMHI-RCA4@IPSL-IPSL-CM5A-MR	Swedish Meteorological and Hydrological Institute	regional		+
SMHI-RCA4@MIROC-MIROC5	Swedish Meteorological and Hydrological Institute	regional	+	+
SMHI-RCA4@MOHC-HadGEM2-ES	Swedish Meteorological and Hydrological Institute	regional	+	+
SMHI-RCA4@MPI-M-MPI-ESM-LR	Swedish Meteorological and Hydrological Institute	regional	+	+
SMHI-RCA4@NCC-NorESM1-M	Swedish Meteorological and Hydrological Institute	regional		+
SMHI-RCA4@NOAA-GFDL-GFDL-ESM2M	Swedish Meteorological and Hydrological Institute	regional		+

Table 5. Thermal transmittance of dwelling structural elements and compliance with standards for thermal zones of RT OGUC.

	Modelling	**Compliance RT OGUC**
Roofing – U [W/m²·K]	0.3290	Zone 6
Walls – U [W/m²·K]	0.6294	Zone 6
Floors – U [W/m²·K]	0.2662	Zone 7
Doors – U [W/m²·K]	1.06	—
Hermetically double-glazed windows – U [W/m²·K]	3.16	Zone 7
Maximum glazed surface with respect to vertical thermal envelope [%]	16%	Zone 7

Table 6. Summary table of thermals zones in the principal cities of communes according to the RT OGUC.

Principal city of communes	**Of. Doc. RT OGUC**	**MM5 baseline climate**	**RCP2.6**			**RCP8.5**		
year	1999***	2006**	2020-2035*	2035-2050*	2050-2065*	2020-2035*	2035-2050*	2050-2065*
	Fig. 3	Fig. 10b	Fig. 11a	Fig. 11c	Fig. 11e	Fig. 11b	Fig. 11d	Fig. 11f
Region de La Araucanía								
Angol	4	5-1387	5-1257(-9%)	4-1214(-12%)	4-1203(-13%)	4-1220(-12%)	4-1110(-20%)	3-987(-29%)
Carahue	5	5-1252	4-1129(-10%)	4-1084(-13%)	4-1075(-14%)	4-1094(-13%)	3-992(-21%)	3-871(-30%)
Cholchol	5	5-1307	4-1182(-10%)	4-1139(-13%)	4-1129(-14%)	4-1147(-12%)	4-1045(-20%)	3-923(-29%)
Collipulli	5	5-1423	5-1291(-9%)	5-1250(-12%)	4-1239(-13%)	5-1254(-12%)	4-1145(-20%)	4-1018(-28%)
Cunco	5	6-1932	6-1779(-8%)	6-1730(-10%)	6-1717(-11%)	6-1732(-10%)	6-1600(-17%)	5-1447(-25%)
Curacautín	5	7-2066	6-1913(-7%)	6-1864(-10%)	6-1851(-10%)	6-1865(-10%)	6-1727(-16%)	6-1567(-24%)
Curarrehue	6	7-2733	7-2565(-6%)	7-2510(-8%)	7-2495(-9%)	7-2509(-8%)	7-2357(-14%)	7-2182(-20%)
Ercilla	5	6-1509	5-1374(-9%)	5-1330(-12%)	5-1320(-13%)	5-1334(-12%)	4-1221(-19%)	4-1089(-28%)
Freire	5	5-1328	4-1203(-9%)	4-1162(-13%)	4-1151(-13%)	4-1166(-12%)	4-1063(-20%)	3-941(-29%)
Galvarino	5	5-1377	5-1251(-9%)	4-1208(-12%)	4-1198(-13%)	4-1215(-12%)	4-1111(-19%)	3-985(-28%)
Gorbea	5	5-1385	5-1259(-9%)	4-1217(-12%)	4-1206(-13%)	4-1221(-12%)	4-1116(-19%)	3-991(-28%)
Lautaro	5	5-1452	5-1321(-9%)	5-1279(-12%)	5-1268(-13%)	5-1282(-12%)	4-1171(-19%)	4-1040(-28%)
Loncoche	5	6-1598	5-1464(-8%)	5-1418(-11%)	5-1407(-12%)	5-1422(-11%)	5-1310(-18%)	4-1175(-26%)
Lonquimay	6	7-3021	7-2849(-6%)	7-2793(-8%)	7-2777(-8%)	7-2791(-8%)	7-2632(-13%)	7-2449(-19%)
Los Sauces	4	5-1443	5-1307(-9%)	5-1263(-12%)	5-1251(-13%)	5-1271(-12%)	4-1157(-20%)	4-1026(-29%)
Lumaco	5	5-1403	5-1273(-9%)	4-1229(-12%)	4-1217(-13%)	4-1237(-12%)	4-1128(-20%)	4-1001(-29%)
Melipeuco	6	7-2719	7-2551(-6%)	7-2498(-8%)	7-2482(-9%)	7-2497(-8%)	7-2344(-14%)	7-2165(-20%)
Nueva Imperial	5	5-1260	4-1135(-10%)	4-1092(-13%)	4-1082(-14%)	4-1100(-13%)	3-999(-21%)	3-879(-30%)
Padre Las Casas	5	5-1346	4-1219(-9%)	4-1177(-13%)	4-1167(-13%)	4-1182(-12%)	4-1077(-20%)	3-954(-29%)
Perquenco	5	5-1479	5-1346(-9%)	5-1303(-12%)	5-1292(-13%)	5-1306(-12%)	4-1195(-19%)	4-1062(-28%)
Pitrufquén	5	5-1333	4-1209(-9%)	4-1167(-12%)	4-1157(-13%)	4-1172(-12%)	4-1068(-20%)	3-947(-29%)
Pucón	6	7-2113	6-1955(-7%)	6-1904(-10%)	6-1891(-11%)	6-1905(-10%)	6-1767(-16%)	6-1607(-24%)
Purén	4	5-1461	5-1326(-9%)	5-1280(-12%)	5-1268(-13%)	5-1290(-12%)	4-1176(-20%)	4-1041(-29%)
Renaico	4	5-1390	5-1288(-7%)	4-1245(-10%)	4-1232(-11%)	4-1248(-10%)	4-1140(-18%)	4-1016(-27%)
Saavedra	5	4-1025	3-909(-11%)	3-865(-16%)	3-858(-16%)	3-876(-15%)	3-782(-24%)	2-675(-34%)
Temuco	5	5-1355	4-1228(-9%)	4-1186(-12%)	4-1175(-13%)	4-1190(-12%)	4-1084(-20%)	3-960(-29%)
Teodoro Schmidt	5	4-1208	4-1087(-10%)	4-1043(-14%)	4-1034(-14%)	4-1051(-13%)	3-953(-21%)	3-838(-31%)
Toltén	5	4-1219	4-1097(-10%)	4-1052(-14%)	4-1043(-14%)	4-1061(-13%)	3-962(-21%)	3-847(-31%)
Traiguén	5	5-1444	5-1314(-9%)	5-1270(-12%)	5-1260(-13%)	5-1277(-12%)	4-1169(-19%)	4-1040(-28%)
Victoria	5	6-1538	5-1402(-9%)	5-1358(-12%)	5-1346(-12%)	5-1361(-12%)	4-1246(-19%)	4-1112(-28%)
Vilcún	5	6-1546	5-1409(-9%)	5-1365(-12%)	5-1354(-12%)	5-1367(-12%)	5-1250(-19%)	4-1113(-28%)
Villarrica	5	6-1560	5-1421(-9%)	5-1377(-12%)	5-1366(-12%)	5-1379(-12%)	5-1261(-19%)	4-1124(-28%)
Region de Los Ríos								
Corral	5	5-1395	5-1266(-9%)	4-1220(-13%)	4-1210(-13%)	4-1230(-12%)	4-1126(-19%)	4-1003(-28%)
Futrono	5	7-2019	6-1864(-8%)	6-1812(-10%)	6-1801(-11%)	6-1817(-10%)	6-1688(-16%)	6-1533(-24%)
La Unión	5	6-1571	5-1437(-9%)	5-1390(-12%)	5-1380(-12%)	5-1398(-11%)	5-1289(-18%)	4-1160(-26%)
Lago Ranco	6	6-1920	6-1769(-8%)	6-1718(-11%)	6-1707(-11%)	6-1723(-10%)	6-1600(-17%)	5-1450(-24%)
Lanco	5	6-1538	5-1404(-9%)	5-1358(-12%)	5-1347(-12%)	5-1363(-11%)	5-1252(-19%)	4-1120(-27%)
Los Lagos	5	6-1620	5-1485(-8%)	5-1438(-11%)	5-1427(-12%)	5-1444(-11%)	5-1333(-18%)	4-1199(-26%)
Máfil	5	5-1421	5-1291(-9%)	4-1246(-12%)	4-1236(-13%)	5-1253(-12%)	4-1148(-19%)	4-1024(-28%)
S.J. de la Mariquina	5	5-1399	5-1270(-9%)	4-1226(-12%)	4-1215(-13%)	4-1232(-12%)	4-1128(-19%)	4-1004(-28%)
Paillaco	5	6-1682	6-1543(-8%)	5-1495(-11%)	5-1484(-12%)	6-1501(-11%)	5-1387(-18%)	5-1252(-26%)
Panguipulli	5	6-1928	6-1781(-8%)	6-1731(-10%)	6-1720(-11%)	6-1735(-10%)	6-1608(-17%)	5-1455(-25%)
Rio Bueno	5	6-1602	5-1466(-8%)	5-1418(-11%)	5-1409(-12%)	5-1425(-11%)	5-1315(-18%)	4-1184(-26%)
Valdivia	5	5-1405	5-1276(-9%)	4-1231(-12%)	4-1220(-13%)	4-1239(-12%)	4-1136(-19%)	4-1013(-28%)

Region de Los Lagos								
Ancud	6	5-1286	4-1157(-10%)	4-1108(-14%)	4-1100(-14%)	4-1124(-13%)	4-1027(-20%)	3-913(-29%)
Calbuco	6	4-1249	4-1106(-11%)	4-1056(-15%)	4-1048(-16%)	4-1071(-14%)	3-967(-23%)	3-847(-32%)
Castro	6	5-1442	5-1306(-9%)	5-1253(-13%)	4-1244(-14%)	5-1272(-12%)	4-1169(-19%)	4-1052(-27%)
Chaitén	6	7-2096	6-1930(-8%)	6-1866(-11%)	6-1859(-11%)	6-1887(-10%)	6-1755(-16%)	6-1601(-24%)
Chonchi	6	5-1373	4-1242(-10%)	4-1190(-13%)	4-1183(-14%)	4-1209(-12%)	4-1110(-19%)	3-997(-27%)
Cochamó	6	7-2572	7-2407(-6%)	7-2347(-9%)	7-2337(-9%)	7-2358(-8%)	7-2219(-14%)	7-2051(-20%)
Curaco de Vélez	6	5-1251	4-1118(-11%)	4-1067(-15%)	4-1059(-15%)	4-1084(-13%)	3-984(-21%)	3-870(-30%)
Dalcahue	6	5-1307	4-1175(-10%)	4-1124(-14%)	4-1116(-15%)	4-1141(-13%)	4-1041(-20%)	3-926(-29%)
Fresia	6	6-1818	6-1674(-8%)	6-1620(-11%)	6-1610(-11%)	6-1635(-10%)	6-1519(-16%)	5-1380(-24%)
Frutillar	6	6-1677	6-1536(-8%)	5-1485(-11%)	5-1475(-12%)	5-1496(-11%)	5-1383(-18%)	4-1248(-26%)
Futaleufú	7	7-3940	7-3758(-5%)	7-3685(-6%)	7-3678(-7%)	7-3705(-6%)	7-3553(-10%)	7-3372(-14%)
Hualaihué	6	6-1633	5-1471(-10%)	5-1414(-13%)	5-1407(-14%)	5-1431(-12%)	5-1311(-20%)	4-1171(-28%)
Llanquihue	6	6-1621	5-1480(-9%)	5-1428(-12%)	5-1419(-12%)	5-1440(-11%)	5-1329(-18%)	4-1195(-26%)
Los Muermos	6	6-1662	6-1520(-9%)	5-1466(-12%)	5-1457(-12%)	5-1481(-11%)	5-1369(-18%)	4-1235(-26%)
Maullín	6	5-1300	4-1170(-10%)	4-1119(-14%)	4-1111(-15%)	4-1134(-13%)	4-1033(-21%)	3-916(-30%)
Osorno	5	6-1599	5-1465(-8%)	5-1416(-11%)	5-1406(-12%)	5-1424(-11%)	5-1317(-18%)	4-1189(-26%)
Palena	7	7-3503	7-3320(-5%)	7-3247(-7%)	7-3239(-8%)	7-3267(-7%)	7-3115(-11%)	7-2937(-16%)
Puerto Montt	6	5-1489	5-1346(-10%)	5-1295(-13%)	5-1287(-14%)	5-1308(-12%)	4-1201(-19%)	4-1072(-28%)
Puerto Octay	6	6-1687	6-1546(-8%)	5-1495(-11%)	5-1485(-12%)	6-1505(-11%)	5-1393(-17%)	5-1257(-25%)
Puerto Varas	6	6-1595	5-1453(-9%)	5-1401(-12%)	5-1392(-13%)	5-1414(-11%)	5-1303(-18%)	4-1171(-27%)
Puqueldón	6	5-1290	4-1160(-10%)	4-1109(-14%)	4-1102(-15%)	4-1126(-13%)	4-1029(-20%)	3-918(-29%)
Purranque	6	6-1763	6-1621(-8%)	6-1569(-11%)	6-1558(-12%)	6-1579(-10%)	5-1464(-17%)	5-1328(-25%)
Puyehue (Entre Lagos)	6	7-2039	6-1886(-8%)	6-1833(-10%)	6-1821(-11%)	6-1840(-10%)	6-1714(-16%)	6-1560(-23%)
Queilén	6	5-1291	4-1159(-10%)	4-1106(-14%)	4-1100(-15%)	4-1126(-13%)	4-1025(-21%)	3-912(-29%)
Quellón	6	5-1308	4-1177(-10%)	4-1124(-14%)	4-1118(-15%)	4-1145(-12%)	4-1046(-20%)	3-936(-28%)
Quemchi	6	4-1187	4-1057(-11%)	4-1008(-15%)	4-1000(-16%)	4-1023(-14%)	3-925(-22%)	3-811(-32%)
Quínchao	6	4-1220	4-1084(-11%)	4-1031(-15%)	4-1024(-16%)	4-1049(-14%)	3-947(-22%)	3-831(-32%)
Rio Negro	6	6-1715	6-1574(-8%)	6-1523(-11%)	6-1512(-12%)	6-1533(-11%)	5-1421(-17%)	5-1288(-25%)
San Juan de la Costa (Puaucho)	6	6-1654	6-1517(-8%)	5-1468(-11%)	5-1457(-12%)	5-1478(-11%)	5-1368(-17%)	4-1235(-25%)
San Pablo	5	6-1581	5-1446(-9%)	5-1398(-12%)	5-1389(-12%)	5-1405(-11%)	5-1296(-18%)	4-1167(-26%)

*Green = no change (thermal zone same as period of baseline climate), yellow = change of 1 thermal zone, orange = change of 2 thermal zones. Column information structure: *thermal zone number – HDD15°C value – % of change of HDD15°C in comparison with baseline climate; ** thermal zone number – HDD15°C value; *** thermal zone number.*

Table 7. Summary of changes of expected thermal zones in cities compared to thermal zones of the official RT OGUC document (Fig. 3).

		2020-2035				2035-2050				2050-2065			
		RCP2.6		RCP8.5		RCP2.6		RCP8.5		RCP2.6		RCP8.5	
		Nº of cities	Change of zones (Nº of cities)	No. of cities	Change of zones (Nº of cities)	Nº of cities	Change of zones (Nº of cities)	Nº of cities	Change of zones (Nº of cities)	Nº of cities	Change of zones (Nº of cities)	Nº of cities	Change of zones (Nº of cities)
Change to colder zone	Change of 1 thermal zone	13 (18%)	4⇒5(4) 5⇒6(5) 6⇒7(4)	11 (15%)	4⇒5(2) 5⇒6(5) 6⇒7(4)	10 (13.5%)	4⇒5(2) 5⇒6(4) 6⇒7(4)	8 (11%)	5⇒6(4) 6⇒7(4)	10 (13.5%)	4⇒5(2) 5⇒6(4) 6⇒7(4)	6 (8%)	5⇒6(2) 6⇒7(4)
No change of zone		35 (47%)	5(22) 6(11) 7(2)	28 (38%)	4(2) 5(16) 6(8) 7(2)	27 (36.5%)	4(2) 5(16) 6(7) 7(2)	21 (28%)	4(4) 5(10) 6(5) 7(2)	26 (35%)	4(2) 5(15) 6(7) 7(2)	11 (15%)	4(3) 5(3) 6(3) 7(2)
Change to warmer thermal zone	Change of 1 thermal zone	14 (19%)	5⇒4(9) 6⇒5(5)	23 (31%)	5⇒4(15) 6⇒5(8)	25 (34%)	5⇒4(16) 6⇒5(9)	27 (36.5%)	5⇒4(18) 6⇒5(9)	25 (34%)	5⇒4(17) 6⇒5(8)	26 (35%)	4⇒3(1) 5⇒4(20) 6⇒5(5)
	Change of 2 thermal zone	12 (16%)	5⇒3(1) 6⇒4(11)	12 (16%)	5⇒3(1) 6⇒4(11)	12 (16%)	5⇒3(1) 6⇒4(11)	14 (19%)	5⇒3(5) 6⇒4(9)	13 (17.5%)	5⇒3(1) 6⇒4(12)	19 (26%)	5⇒3(11) 6⇒4(8)
	Change of 3 thermal zone							4 (5.5%)	6⇒3(4)			12 (16%)	5⇒2(1) 6⇒3(11)

Table 8. Heating EC (kWh/m^2/year) in cities for baseline climate period and in the future 2050–2065.

Cap. city of comm.	EC baseline climate 2006 (Fig. 12)	EC 2050-2065 RCP2.6/RCP8.5 (Fig. 15c)	ΔEC RCP2.6/RCP8.5	Cap. city of comm.	EC baseline climate 2006 (Fig. 12)	EC 2050-2065 RCP2.6/RCP8.5 (Fig. 15c)	ΔEC RCP2.6/RCP8.5
Angol	96	84/69	-13%/-29%	Los Lagos	108	95/80	-12%/-26%
Carahue	82	71/57	-14%/-30%	Máfil	98	85/71	-13%/-28%
Cholchol	91	79/64	-14%/-29%	S.J. de la Mariquina	95	83/68	-13%/-28%
Collipulli	99	86/71	-13%/-28%	Paillaco	112	99/83	-12%/-26%
Cunco	120	107/90	-11%/-25%	Panguipulli	121	108/91	-11%/-25%
Curacautín	130	116/98	-10%/-24%	Rio Bueno	103	91/76	-12%/-26%
Curarrehue	190	174/152	-9%/-20%	Valdivia	93	81/67	-13%/-28%
Ercilla	102	89/73	-13%/-28%	Ancud	79	67/56	-14%/-29%
Freire	92	80/65	-13%/-29%	Calbuco	74	62/50	-16%/-32%
Galvarino	95	83/68	-13%/-28%	Castro	88	76/64	-14%/-27%
Gorbea	96	84/69	-13%/-28%	Chaitén	120	106/91	-11%/-24%
Lautaro	98	85/70	-13%/-28%	Chonchi	85	73/62	-14%/-27%
Loncoche	106	94/78	-12%/-26%	Cochamó	167	152/133	-9%/-20%
Lonquimay	223	205/181	-8%/-19%	Curaco de Vélez	75	64/52	-15%/-30%
Los Sauces	99	86/71	-13%/-29%	Dalcahue	79	68/56	-15%/-29%
Lumaco	97	84/69	-13%/-29%	Fresia	108	95/82	-11%/-24%
Melipeuco	189	173/151	-9%/-20%	Frutillar	104	91/77	-12%/-26%
Nueva Imperial	87	75/61	-14%/-30%	Futaleufú	286	267/245	-7%/-14%
Padre Las Casas	93	80/66	-13%/-29%	Hualaihué	90	78/65	-14%/-28%
Perquenco	98	86/71	-13%/-28%	Llanquihue	99	87/73	-12%/-26%
Pitrufquén	93	81/66	-13%/-29%	Los Muermos	97	85/72	-12%/-26%
Pucón	130	116/99	-11%/-24%	Maullín	77	66/55	-15%/-30%
Purén	98	85/70	-13%/-29%	Osorno	101	89/75	-12%/-26%
Renaico	97	86/71	-11%/-27%	Palena	243	225/204	-8%/-16%
Saavedra	65	55/43	-16%/-34%	Puerto Montt	89	77/64	-14%/-28%
Temuco	93	81/66	-13%/-29%	Puerto Octay	104	92/78	-12%/-26%
Teodoro Schmidt	82	71/57	-14%/-31%	Puerto Varas	97	85/71	-13%/-27%
Toltén	83	71/57	-14%/-31%	Puqueldón	80	68/57	-15%/-29%
Traiguén	98	85/70	-13%/-28%	Purranque	109	97/82	-12%/-25%
Victoria	101	88/73	-12%/-28%	Puyehue	124	111/95	-11%/-23%
Vilcún	99	86/71	-12%/-28%	Queilén	80	68/56	-15%/-29%
Villarrica	100	88/72	-12%/-28%	Quellón	83	71/59	-15%/-28%
Corral	87	76/63	-13%/-28%	Quemchi	73	62/50	-16%/-32%
Futrono	123	110/94	-11%/-24%	Quínchao	72	60/49	-16%/-32%
La Unión	100	88/74	-12%/-26%	Rio Negro	107	94/80	-12%/-25%
Lago Ranco	115	102/87	-11%/-24%	San Juan de la Costa	100	88/75	-12%/-25%
Lanco	103	91/75	-12%/-27%	San Pablo	101	89/75	-12%/-26%

GRAPHICAL ABSTRACT

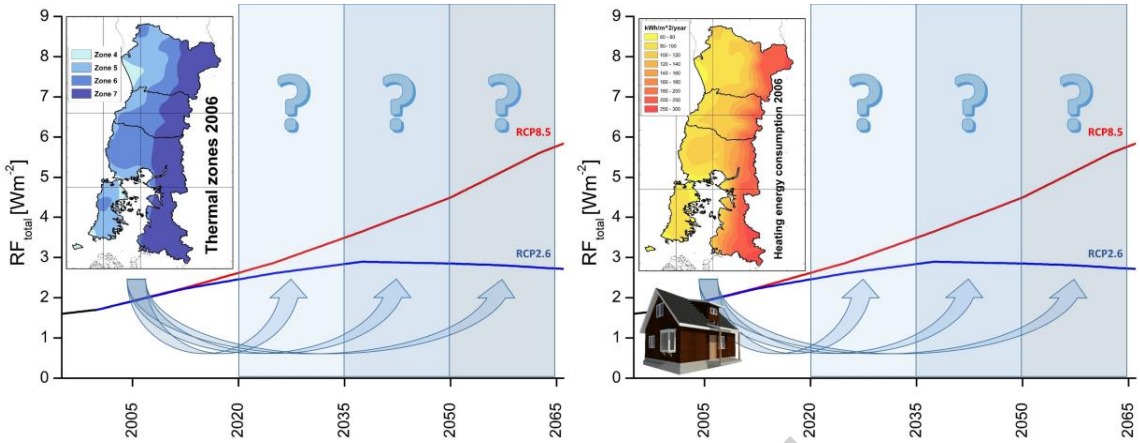

Credit Author Statement

Konstantin Verichev
Conceptualization; Methodology; Software; Validation; Formal analysis; Investigation; Resources; Data Curation; Writing - Original Draft; Visualization

Montserrat Zamorano
Conceptualization; Methodology; Validation; Formal analysis; Investigation; Writing - Review & Editing; Visualization; Supervision

Manuel Carpio
Conceptualization; Methodology; Validation; Formal analysis; Investigation; Resources; Writing - Review & Editing; Visualization; Supervision; Project administration; Funding acquisition

Declaration of interests

X The authors declare that they have no known competing financial interests or personal relationships that could have appeared to influence the work reported in this paper.

☐The authors declare the following financial interests/personal relationships which may be considered as potential competing interests: